OXFORD

Cerebral Cortex, 2023, 1–24
https://doi.org/10.1093/cercor/bhad333
Original Article

Visual, delay, and oculomotor timing and tuning in macaque dorsal pulvinar during instructed and free choice memory saccades

Lukas Schneider[1,2], Adan-Ulises Dominguez-Vargas[1,3], Lydia Gibson[1,2], Melanie Wilke[1,2,4,5], Igor Kagan[1,5,*]

[1]Decision and Awareness Group, Cognitive Neuroscience Laboratory, German Primate Center, Leibniz Institute for Primate Research, Kellnerweg 4, Goettingen 37077, Germany,
[2]Department of Cognitive Neurology, University Medical Center Göttingen, Robert-Koch-Str. 40, Goettingen 37075, Germany,
[3]Département de Neurosciences, Faculté de Médecine, Université de Montréal, QC H3C 3J7, Canada,
[4]DFG Center for Nanoscale Microscopy & Molecular Physiology of the Brain (CNMPB), Robert-Koch-Str. 40, Göttingen 37075, Germany,
[5]Leibniz ScienceCampus Primate Cognition, Kellnerweg 4, Goettingen 37077, Germany

*Corresponding author: German Primate Center, Leibniz Institute for Primate Research Kellnerweg 4, Goettingen, 37077, Germany. E-mail: ikagan@dpz.eu

Causal perturbations suggest that primate dorsal pulvinar plays a crucial role in target selection and saccade planning, though its basic neuronal properties remain unclear. Some functional aspects of dorsal pulvinar and interconnected frontoparietal areas—e.g. ipsilesional choice bias after inactivation—are similar. But it is unknown if dorsal pulvinar shares oculomotor properties of cortical circuitry, in particular delay and choice-related activity. We investigated such properties in macaque dorsal pulvinar during instructed and free-choice memory saccades. Most recorded units showed visual (12%), saccade-related (30%), or both types of responses (22%). Visual responses were primarily contralateral; diverse saccade-related responses were predominantly post-saccadic with a weak contralateral bias. Memory delay and pre-saccadic enhancement was infrequent (11–9%)—instead, activity was often suppressed during saccade planning (25%) and further during execution (15%). Surprisingly, only few units exhibited classical visuomotor patterns combining cue and continuous delay activity or pre-saccadic ramping; moreover, most spatially-selective neurons did not encode the upcoming decision during free-choice delay. Thus, in absence of a visible goal, the dorsal pulvinar has a limited role in prospective saccade planning, with patterns partially complementing its frontoparietal partners. Conversely, prevalent visual and post-saccadic responses imply its participation in integrating spatial goals with processing across saccades.

Key words: eye movements; memory saccades; oculomotor decision; spatial choice selectivity.

Introduction

Visual information is crucial for guiding primate behavior. To gather this information, primates make saccadic eye movements toward locations of interest, allowing the fovea to obtain a better spatial resolution of these parts of the environment (Boi et al. 2017). Since eye movements are typically guided by visual inputs, it is not surprising that numerous cortical and subcortical regions show both visually-driven responses as well as saccade-related activity. To study visuomotor transformations underlying conversion of visual inputs into oculomotor actions, a classical memory-guided saccade task that allows separating visual, intervening delay and motor-related activity has been used extensively (Hikosaka and Wurtz 1983). With this task it has been shown that besides transient visually-evoked and motor-related responses, many neurons in oculomotor structures such as lateral intraparietal area (LIP), frontal eye fields (FFE), dorsal lateral prefrontal cortex (dlPFC), superior colliculus (SC), mediodorsal thalamus (MD), and central oculomotor thalamus show persistent delay activity. This activity links the visual input to an eventual motor output, and is considered a signature of many cognitive signals such as working memory, sustained attention, motor preparation, and evolving decision (Bruce and Goldberg 1985; Barash et al. 1991a; Funahashi et al. 1991; Basso and Wurtz 1998; Watanabe and Funahashi 2004a, 2007; Wyder et al. 2004, 2004; Lawrence et al. 2005; Kagan et al. 2010; Constantinidis et al. 2018).

Another important aspect of sensorimotor transformation concerns the continuity of visual experience and action guidance during a normal fixation-saccade cycle. Visual inputs enter the brain in eye-centered, retinotopic coordinates, but every saccade changes these representations, necessitating a mechanism for maintaining visual stability across saccades (Wurtz et al. 2011a). It has been suggested that a corollary discharge (or efference copy) pathway involving SC, MD, and FEF is one important contributor enabling anticipation of movement consequences and saccade suppression (Wurtz et al. 2011a). The remapping of receptive fields around saccades in FEF and LIP is another related phenomenon thought to support visual stability (Bisley and Goldberg 2010; Mirpour and Bisley 2016). In addition to these prospective mechanisms manifesting prior to or during saccades, post-saccadic responses might also contribute to saccadic suppression, as well as to saccade updating and error processing (Zhou et al. 2016b).

Due to its widespread bidirectional connectivity to a host of visual and oculomotor cortical areas, the thalamic pulvinar is another likely candidate for mediating distributed mechanisms

Received: July 22, 2022. **Revised:** July 16, 2023. **Accepted:** August 16, 2023

linking visual inputs to processing that spans across eye movements (Grieve et al. 2000; Guillery and Sherman 2002; Wilke et al. 2010b; Berman and Wurtz 2011; Saalmann and Kastner 2015). Distinct pulvinar subdivisions might however contribute differently to these functions. Several studies have motivated a functional distinction between the ventral and the dorsal pulvinar aspects, based either on distinctive patterns of anatomical (Stepniewska et al. 1994; Kaas and Lyon 2007) and functional/effective connectivity (Arcaro et al. 2015, 2018; Kagan et al. 2021), or based on dissimilar functional properties within the same anatomically-defined subdivision, e.g. leading to further division of the lateral pulvinar into dorsal and ventral parts (Petersen et al. 1985; Baldwin et al. 2017). The ventral pulvinar (vPul, encompassing inferior pulvinar and ventral part of lateral pulvinar) is retinotopically organized and has strong connections to visual cortices (Kaas and Baldwin 2020). Ventral pulvinar neurons respond to contralateral visual stimuli but show weak or no pre-saccadic activity—most eye movement-related responses are peri- or post-saccadic (Petersen et al. 1985; Robinson et al. 1986; Berman and Wurtz 2011). In particular, the inferior pulvinar has been identified as a part of pathway from superficial layers of SC to cortical area MT that carries saccadic suppression signals (Berman and Wurtz 2011), while the SC–ventral lateral pulvinar pathway is involved in mediating the residual vision (blindsight) after V1 lesions (Kinoshita et al. 2019).

The dorsal pulvinar (dPul, encompassing medial pulvinar and dorsal part of lateral pulvinar) is reciprocally interconnected with posterior parietal and prefrontal cortices subserving attentional and sensorimotor functions, in particular LIP, area 7, FEF, dlPFC, and posterior cingulate cortex (PCC; Bos and Benevento 1975; Trojanowski and Jacobson 1976; Hardy and Lynch 1992; Gutierrez et al. 2000; Dean et al. 2004; Saalmann and Kastner 2011; Bridge et al. 2016; Bourgeois et al. 2020; Homman-Ludiye et al. 2020). Unlike the ventral pulvinar, the dorsal pulvinar does not follow clear retinotopic organization (Benevento and Miller 1981; Petersen et al. 1987; Benevento and Port 1995; Arcaro et al. 2015). Only few studies investigated visuomotor neuronal properties in the macaque dorsal pulvinar (in particular the medial part) using oculomotor tasks. Robinson, Petersen, and colleagues (Petersen et al. 1985; Robinson et al. 1986) assessed responses to visually-guided saccades in the lateral part of the dorsal pulvinar (PLdm, denoted Pdm in the original studies). They showed that some Pdm neurons fired in association with eye movements, are crudely tuned for saccade direction and amplitude, and exhibit modulation of visual responses when stimuli are attended or serve as a saccade target. Another study showed that the visual responsivity to stimuli in the receptive field is reduced in the lateral dorsal pulvinar when monkeys attend to the central fixation, further suggesting the importance of behavioral relevance and involvement of Pdm/PLdm in selective visual attention (Bender and Youakim 2001).

To our knowledge, only one study prior to our work investigated neurons in the dorsal pulvinar with the memory-guided saccade task (Benevento and Port 1995). The main focus of this prior study was on color and pattern processing; the comparison of visually-guided and memory-guided task responses in a small sample indicated that stimulus-unrelated activity was post-saccadic. Surprisingly, visual target-related responses were reported during visually-guided but not memory-guided saccades, and the delay activity was not addressed. The authors suggested that only when the stimulus serves as an *immediate* saccade target the visual response takes place, although it is not the pattern typically observed in the frontoparietal cortical areas. Finally, we recently have shown that dPul neurons carry information about static eye position and combine spatial encoding in eye-centered and non-retinocentric coordinates, potentially contributing to coordinate frame transformations (Schneider et al. 2019).

In contrast to paucity of single neuron studies on oculomotor processing and target selection in the dorsal pulvinar, more is known about consequences of its causal perturbation. While primary sensory and oculomotor functions are largely spared (Ungerleider and Christensen 1977; Bender and Butter 1987; Bender and Baizer 1990; Wilke et al. 2013), dPul inactivation or microstimulation affects saccadic reaction times (RTs) and biases hemifield-specific spatial exploration and target selection, especially in conditions of a free choice (Wilke et al. 2010b; Wilke et al. 2013; Dominguez-Vargas et al. 2017). Inactivation of the lateral part of the dorsal pulvinar also impairs contralateral attentional orienting (Petersen et al. 1987; Desimone et al. 1990) and perceptual decision confidence (Komura et al. 2013). It is not clear, however, whether the transformation from visual processing to motor actions is implemented already within the dPul at the level of individual neurons, or these transformations are only taking place in the interconnected cortical circuitry. Furthermore, it is not known if dPul neurons show delay period or pre-saccadic spatial choice selectivity, similar to frontoparietal cortex (Coe et al. 2002; Watanabe and Funahashi 2007) and other higher-order thalamic nuclei such as central and mediodorsal thalamus (Wyder et al. 2004; Watanabe and Funahashi 2004a; Costello et al. 2015).

In a recent electrical microstimulation study of choice behavior in the dorsal and ventral pulvinar (Dominguez-Vargas et al. 2017), we provided initial electrophysiological assessment of microstimulation sites in dPul (mostly in the medial pulvinar). A comprehensive characterization of dPul using a classical memory-guided saccade task, crucial for understanding basic visuomotor processing, is still lacking. To address this gap, here our first aim was to examine the temporal dynamics of enhancement, suppression, and spatial tuning of visual and saccade-related activity in dPul, and quantify their interdependence. Second, we aimed to explore the relationship between pulvinar activity and prospective visuomotor transformations during motor preparation by analyzing the delay period activity. Given the significant impact of pulvinar perturbations on spatial choices, we also tested the hypothesis that dPul neurons encode upcoming decisions in free-choice two-target trials.

Materials and methods

All experimental procedures were conducted in accordance with the European Directive 2010/63/EU, the corresponding German law governing animal welfare, and German Primate Center institutional guidelines. The procedures were approved by the responsible government agency ("Niedersächsisches Landesamt für Verbraucherschutz und Lebensmittelsicherheit" - Lower Saxony State Office for Consumer Protection and Food Safety, LAVES, Oldenburg, Germany; permit 3392-42502-04-13/1100). The animals were pair- or group-housed in facilities of the German Primate Center in accordance with all applicable German and European regulations. The facility provides the animals with an enriched environment, including a multitude of toys and wooden structures (Calapai et al. 2017; Berger et al. 2018), natural as well as artificial light and access to outdoor space, exceeding the size requirements of European regulations, and a rich diet including primate biscuits, fruit, and vegetables.

Animal preparation

Two adult male rhesus monkeys (*Macaca mulatta*) C and L weighing 8 and 9 kg, respectively, were used. Monkeys were pair-housed with other males in two enclosures (23.3 and 21.3 m^3) conjoined by an overhead tunnel. In an initial surgery, monkeys were implanted with a magnetic resonance imaging (MRI) compatible polyetheretherketone (PEEK) headpost embedded in a bone cement headcap (Palacos with Gentamicin, BioMet, USA) anchored by ceramic screws (Rogue Research, Canada), under general anesthesia and aseptic conditions. MR-visible markers were embedded in the headcap to aid the planning of the chamber in stereotaxic space with the MR-guided stereotaxic navigation software Planner (https://github.com/shayo/Planner) (Ohayon and Tsao 2012). A separate surgery was performed to implant PEEK MRI-compatible chamber(s) (inside diameter 22 mm) allowing access to the pulvinar (Monkey C, right hemisphere: center at 0.5A/14.5R mm, tilted -11P/27R degrees; Monkey L, right hemisphere: center at -3.12P/20.2R mm, tilted -18P/37R degrees; Monkey L, left hemisphere: center at -3P/20L, tilted -18P/-38L; the coordinates are relative to stereotaxic zero, A—anterior, P—posterior, L—left, R—right; the tilts are relative to the vertical axis normal to stereotaxic plane: P—posterior, top of the chamber tilted toward the back of the head, L/R—left/right, top of the chamber tilted toward the corresponding ear). After confirming chamber positioning with a post-surgical MRI, a partial craniotomy was made inside the chamber. The exposed dura was covered with a silicone elastomer (Kwik-sil, World Precision Instruments, USA) to reduce granulation tissue growth and dura thickening.

MRI imaging

Monkeys were scanned in a 3T MRI scanner (Siemens Magnetom TIM Trio). Full-head T1-weighted scans (3D magnetization-prepared rapid gradient-echo, MPRAGE, 0.5 mm isometric) were acquired before and after chamber implantation, in awake (monkey C) or anaesthetized (monkey L) state, using either a built-in gradient body transmit coil and a custom single loop receive coil, or a custom single loop transmit and four-channel receive coil (Windmiller Kolster Scientific, USA).

In addition to pre- and post-implantation scans, similar T1-weighted scans as well as T2-weighted (rapid acquisition with relaxation enhancement, RARE, 0.25 mm in plane resolution, 1 mm slice thickness) scans were periodically acquired during the course of experiments, either in awake (monkey C) or sedated (monkey L) state, to confirm electrode positioning. These images were acquired with the chamber and a custom-made MR-compatible polyetherimide (Ultem) grid (0.8 mm hole spacing, 0.45 mm hole diameter) filled with gadolinium (Magnevist, Bayer, Germany)/saline solution (proportion 1:200), with tungsten rods inserted in predefined grid locations, for alignment purposes. The electrode penetration trajectory and the recording depth was visualized using platinum-iridium electrodes (FHC Inc., USA, 100 mm length platinum-iridium 125 μm thick core, initial 2 cm glass-coated, total thickness of 230 μm including polyamide tubing coating, UEPLEFSS (UEIK1)), advanced by an MRI-compatible custom-made plastic XYZ manipulator drive through the corresponding grid hole. For the dura penetration, the electrode was protected by a custom-made MRI-compatible fused silica guide tube (320 μm inner diameter, 430 μm outer diameter, Polymicro Technologies, USA). A stopper (530 μm inner diameter, 665 μm outer diameter, 23 gauge MicroFil, World Precision Instruments, USA) ensured that the guide tube only penetrated the dura and minimally the cortex below. Prior to penetration, the electrode tip was aligned to the guide tube tip and was held in place by a drop of melted Vaseline. The guide tube was filled with sterile silicone oil prior to electrode insertion, to ensure smooth electrode travel and to prevent the backflow of cerebrospinal fluid. T1- and T2-weighted scans were co-registered and transformed into "chamber normal" (aligned to the chamber vertical axis) and to anterior commissure-posterior commissure space for electrode targeting and visualization in BrainVoyagerQX (Brain Innovation, Netherlands) and Planner (Ohayon and Tsao 2012; Kagan et al. 2021).

Electrophysiological recordings

Dorsal pulvinar neuronal activity was recorded with up to four individually-movable single platinum-tungsten (95–5%) quartz glass-insulated electrodes with impedance ranging from 1 to 1.9 MΩ for monkey C and 1 to 3.5 MΩ for monkey L, using a chamber-mounted 5-channel Mini Matrix microdrive (Thomas Recording, Germany). Single custom-made stainless steel guide tubes (27 gauge), made from Spinocan spinal needle (B. Braun Melsungen AG, Germany) filled with silicone oil (Thomas Recording), with a metal funnel attached to the microdrive nozzle were used to protect electrodes during grid insertion and dura penetration. A reference tungsten rod or a silver wire was placed in the chamber filled with saline, and was connected to the chassis of the drive. Neuronal signals were amplified (×20 headstage, Thomas Recording; ×5-, 128-, or 32-channel PZ2 preamplifier, Tucker-Davis Technologies, USA), digitized at 24 kHz and 16-bit resolution, and sent via fiber optics to an RZ2 BioAmp Processor (Tucker-Davis Technologies, USA) for online filtering (300–5,000 Hz bandpass), display and storage on a hard drive together with behavioral and timing data streams.

Behavioral tasks

Monkeys sat in a dark room in custom-made primate chairs with their heads restrained 32 or 29 cm away from a 27" LED display (60 Hz refresh rate, model HN274H, Acer Inc. USA), covering a range of 84 × 53 visual degrees for monkey C and 91 × 59 for monkey L. The gaze position of the right eye was monitored at 220 Hz using an MCU02 ViewPoint infrared eyetracker (Arrington Research Inc. USA). Eye position was calibrated using linear gains and offsets for horizontal and vertical axes, using visually-guided saccades. All stimulus presentation and behavioral control tasks were programmed in MATLAB and the Psychophysics Toolbox (Brainard 1997), using a custom monkeypsych toolbox (https://github.com/dagdpz/monkeypsych).

Memory-guided saccade task

A trial started with the onset of the fixation point of 1° diameter. After the gaze fixation was acquired and held within a 5° radius for 500 ms, either one peripheral 1° diameter cue (instructed trials) or two peripheral cues (choice trials) were displayed for 300 ms at the location(s) signaling the upcoming saccade target(s). Cues were presented in the left and/or right side(s) of the fixation point, at 12° or 24° absolute eccentricity, with six potential directions relative to the horizontal axis: circular angles counterclockwise 0°, 20°, 160°, 180°, 200°, 340° (resulting in 0°, 4.1°, –4.1°, 8.2°, and –8.2° vertical eccentricity). Monkeys were required to maintain fixation throughout the cue period and the subsequent memory period (1,000 ms), after which the central fixation point disappeared, prompting monkeys to saccade to the remembered instructed location, or to choose one of the two cued

locations, within 500 ms. The fixation offset will be referred to as the Go signal. After a saccade to and fixation inside a 5° radius window around the remembered target location for 100 or 200 ms, the selected target became visible, and after additional 500 ms of peripheral fixation, the trial was completed and a liquid reward was dispensed after a delay of 200 ms. Instructed trials (50%) were interleaved with choice trials (50%), and trial types and target locations were pseudo-randomized. In choice trials the two cues were always presented simultaneously at the same height and provided equal reward. The inter-trial interval for both successful and unsuccessful trials was 2,000–2,500 ms (Fig. 1A).

Visually-guided saccade task

In addition to the memory-guided saccade task, monkeys also performed visually-guided saccades in separate blocks in most of the sessions. In this task, after the initial fixation period the fixation point disappeared and the visual target(s) appeared at the same time, serving as the Go signal. Monkeys had to saccade toward the visible peripheral target and keep fixating it for 500 ms to obtain a liquid reward. Target sizes, colors, and locations were the same as for memory-guided saccades, and trial types and target locations were pseudo-randomized.

Data analysis

Saccade definition

Instantaneous saccade velocity was calculated sample by sample as the square root of the sum of squared interpolated (220 Hz to 1 kHz) and smoothed (12 ms moving average rectangular window) horizontal and vertical eye position traces, and then smoothed again (12 ms moving average rectangular window). Saccade onset was defined as the first eye position change after the go signal that exceeded a velocity threshold of 200°/s; saccade end was defined as the first eye position change below 50°/s after saccade onset. In instructed memory-guided trials, average saccade latency across sessions was 199 ± 2 ms (213 ± 1 ms for monkey C, 190 ± 1 ms for monkey L); average saccade duration 46.2 ± 0.2 ms (47.8 ± 0.2 and 45.2 ± 0.2), average maximum saccade velocity was 619 ± 4°/s (592 ± 4°/s and 636 ± 4°/s). For corrective saccades (small re-fixation saccades after target reappearance), 20°/s and 10°/s were used as onset and end velocity thresholds. Corrective saccades were common in both monkeys (90 ± 2% and 92 ± 1% of all trials), with an average latency of 125 ± 3 ms (138 ± 5 ms and 116 ± 2 ms) after target reappearance and average amplitude of 1.08 ± 0.02° (1.00 ± 0.03° and 1.13 ± 0.02°). All values in this section are session means ± SE, values in parentheses for monkey C and for monkey L separately. For details, see Supplementary Table S1**.**

Datasets and unit selection criteria

All voltage drops that crossed an online visually determined threshold were defined as potential spikes and recorded on the hard drive. Spike sorting was done in Offline Sorter v.3.3.5 (Plexon, USA), using a waveform template algorithm, after manually defining templates by clustering in principle component space using first three principle components, as well as the recording time axis. Based on the inspection of spike shapes, principle component cluster shapes and inter-spike intervals, clusters were categorized as single units, multi-units, and rejected "noise".

In total, 416 single and multi-units were recorded in the dorsal pulvinar (dPul) in 50 sessions during the memory-guided saccade task (monkey C; right hemisphere: 235, monkey L; right hemisphere: 123; left hemisphere: 58). Out of these, 371 units (200—monkey C right dPul, 115—monkey L right dPul, 56—monkey L left dPul) fulfilled analysis selection criteria (stable discriminability across time and acceptable signal-to-noise ratio—assessed by inspection). Out of these 371 units, 322 units (174 monkey C right dPul, 98 monkey L right dPul, 50 monkey L left dPul) were recorded for at least 4 successful instructed trials for each of the 12 targets and were used for further analysis. The median (across units) minimal number of trials per instructed target position was 10 trials (with a range from 4 to 29 trials). Most units (251 out of 322) were recorded for at least 9 trials per target position. The median (across units) average number of trials per position was 18 with a range from 6 to 40 trials.

Out of 322 units accepted for the analysis, 228 units (116 monkey C right dPul, 79 monkey L right dPul, 33 monkey L left dPul) were categorized as well-isolated stable single units. Out of these 228 units, 186 units were also recorded in at least 24 choice trials for each hemifield and used for spatial choice selectivity analysis that only considered single units. All other analyses were performed on single and multi-units together.

The mean firing rate of 228 well-isolated stable single units was 13.4 spikes/s (median: 9.0, SD: 11.7), as compared with 18 spikes/s (median: 11.4, SD: 14.8) for the 73 remaining multi-units, and 14.6 spikes/s across all 322 units (median: 9.7, SD: 12.8).

Out of 322 units analyzed for the memory-guided task, 195 units (101 monkey C right dPul, 54 monkey L right dPul, 40 monkey L left dPul) were also recorded during the visually-guided saccade task. Out of these 195 units, 174 (88 monkey C right dPul, 46 monkey L right dPul, 40 monkey L left dPul) were recorded for at least 4 successful instructed trials for each of the 12 targets. These 174 units were used for comparison between the two tasks. For the instructed vs. choice tuning analysis in the visually-guided task, 137 units with at least 24 choice trials for each hemifield were used.

Epoch definitions

For each trial, and each epoch of interest, firing rates were computed by counting spikes within the epoch and dividing by the epoch duration. The following epochs were analyzed: inter-trial interval (400 to 100 ms before the onset of the central fixation point, corresponding to the fixation acquire), fixation hold (last 300 ms of central fixation), cue onset (60 ms to 160 ms after cue onset), memory (last 300 ms of the memory period), pre-saccadic (100 to 10 ms before saccade onset), peri-saccadic (10 ms before to 50 ms after saccade onset), and post-saccadic (first 150 ms after acquiring the invisible peripheral target) (Fig. 1B). The first two epochs, the inter-trial interval and the fixation hold, were only used for the firing rate normalization (the inter-trial interval firing rate subtraction normalization was only used in Fig. 8A,B).

The cue onset epoch was defined according to findings in the response timing analysis as 100 ms around the enhancement peak, see Fig. 2(D). We did not base our post-saccadic epoch on such analysis, for two reasons. First, the onset of post-saccadic modulation was not as synchronized across units as the cue response (cf. Fig. 2D,E). Second, in some sessions, the target became visible already 100 ms after saccade end, which could lead to confounding visual responses, giving only a short interval for a purely post-saccadic epoch. Instead, we defined the post-saccadic epoch as the first 150 ms after saccade end. In those cases when the target appeared already 100 ms after the saccade end, this epoch would not be contaminated by visual response to the target onset because visual latency of most pulvinar neurons was >50 ms.

To compare firing rates in the target onset/pre-saccadic epoch of the visually-guided saccade task (40–140 ms after target onset/Go signal, termed 'target-pre-sac') to firing rates in the

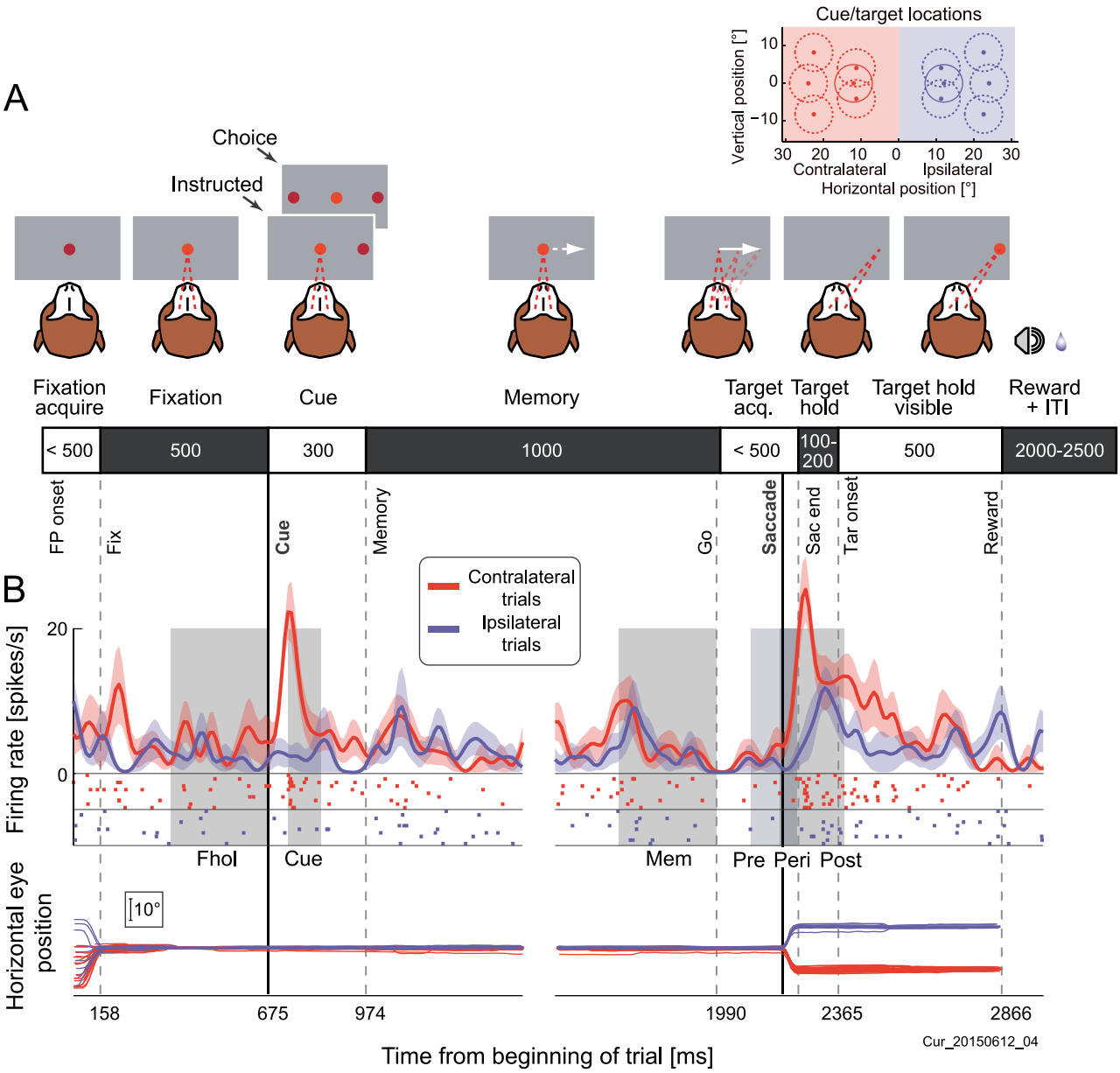

Fig. 1. Memory-guided saccade task and example neuron activity. (A) Task layout. Monkeys had to fixate in the center while one or two cues were flashed peripherally. After a 1 s memory period monkeys had to make a saccade to (one of) the previously cued location(s), and fixate this location until and after the target became visible in order to receive reward. In instructed trials, there was one target; in choice trials, there were two targets. The two targets in choice trials were always presented at the same height and eccentricity and provided equal reward. Inset on the top right shows all cue/target positions and fixation windows; solid fixation windows indicate two positions in trials shown in (B). (B) Raster plots and spike density functions for two example positions, a contralateral (orange) and the opposite ipsilateral (blue) position. Corresponding horizontal eye traces are below. Vertical lines indicate average onset of events across all trials (including other target positions): monkey acquiring fixation (Fix), the cue onset, the cue offset and beginning of the memory period, the offset of the central fixation point (Go), the saccade onset, monkey acquiring the invisible target location (Sac end), the onset of the visible peripheral target (Tar onset), and the end of the trial (Reward). Discontinuous traces indicate two different alignments to cue onset and saccade onset events (continuos lines). Grey boxes mark analyzed epochs: fixation hold (Fhol), cue onset (Cue), memory (Mem), pre-saccadic (Pre), peri-saccadic (Peri), and post-saccadic (Post) (see Materials and Methods).

memory-guided saccade task, two additional corresponding epochs were defined for the memory-guided task: 'cue onset 2' (40–140 ms after cue onset) and 'pre-saccadic 2' (130–30 ms before saccade onset).

Epoch-based spatial tuning and response modulation

Spatial tuning

For each unit, hemifield preference (data from 6 left vs. 6 right hemifield targets) in each epoch was determined in two steps. First, a two-sided permutation test (https://github.com/behinger/permtest, 'conservative' method, 1,000 permutations) was performed to compare firing rates in ipsilateral trials to firing rates in contralateral trials in each epoch. Secondly, the *P*-values derived from permutation tests were corrected for multiple comparison across five epochs of interest using the Benjamini–Hochberg false discovery rate (FDR) procedure (Benjamini and Hochberg 1995) [David Groppe (2023). fdr_bh (https://www.mathworks.com/matlabcentral/fileexchange/27418-fdr_bh), MATLAB Central File Exchange. Retrieved January 16, 2023]. For each epoch, the hemifield with the higher firing rate was marked, if there was a significant difference after multi-comparison correction, at FDR threshold q(FDR)<0.05.

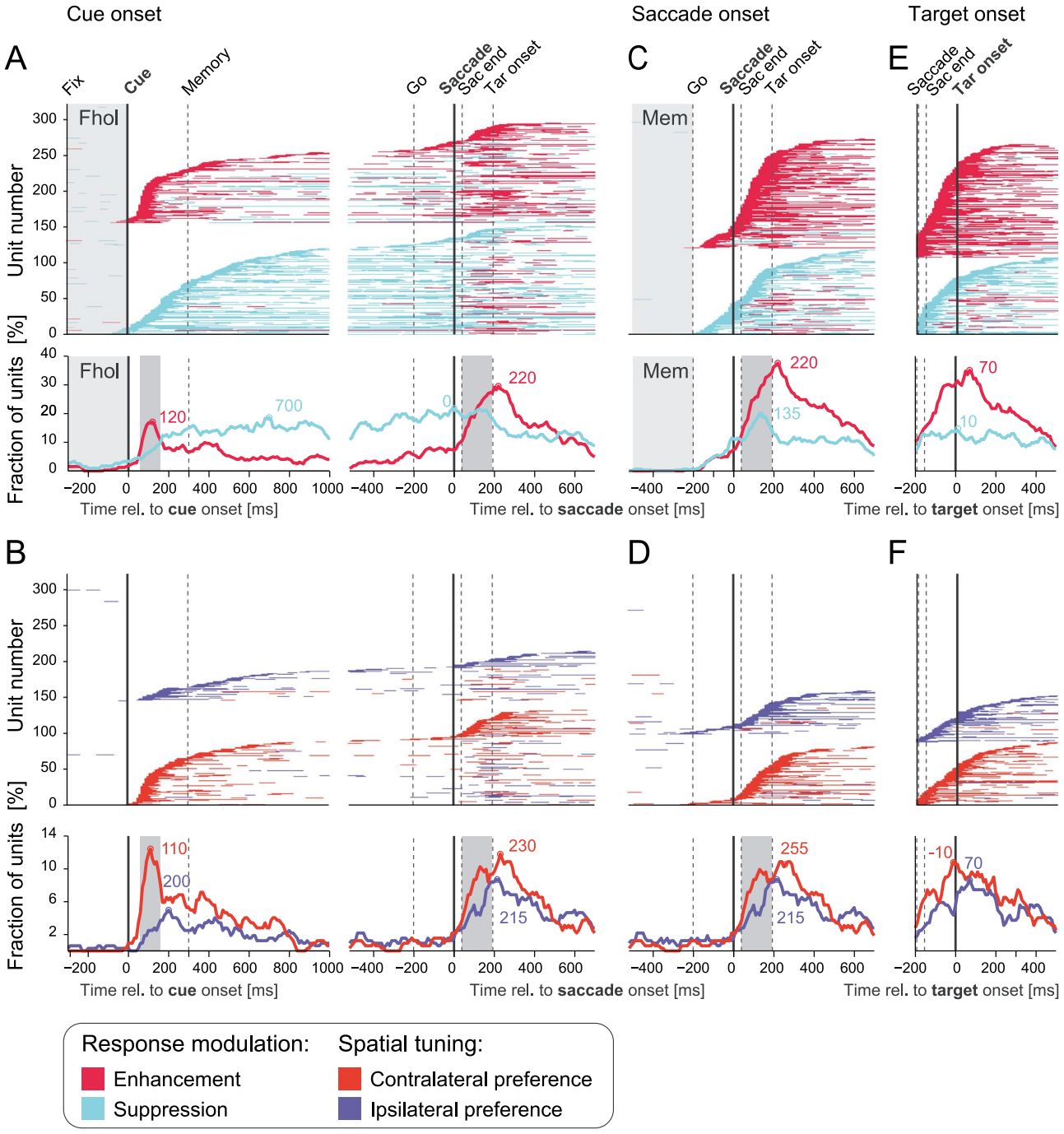

Fig. 2. Response modulation and spatial tuning onsets. (A) Bin-by-bin (10 ms) response modulation for all 322 recorded units. The cluster-based permutation test was used to assess significance, applying a cluster-forming threshold and critical *P*-value both set at $P < 0.05$. Top: units ordered by the significant modulation onset time relative to cue onset. Each horizontal line represents one unit. Response modulation is shown as enhancement (red) or suppression (cyan) relative to the baseline fixation hold epoch (Fhol), indicated by a light gray box. Vertical lines indicate average onset of events across all trials and units. Discontinuous traces indicate two different alignments to cue onset and saccade onset events (continuous vertical lines). Bottom: fraction of units showing enhancement or suppresion per bin. The gray box denotes the cue onset epoch. Colored circles and numbers show the time (relative to alignment event) corresponding to the maximum number of modulated or tuned units. When there were several equal maxima, the respective time points were averaged (as in D, lower panel). (B) Hemifield preference across time for all units recorded (contralateral—orange, ipsilateral—blue). Top: units ordered by significant tuning onset time relative to cue onset. Bottom: fraction of units showing hemifield preference per bin. (C and D) Same as (A) and (B), ordered by modulation/tuning onset relative to saccade, starting 200 ms before saccade onset. Here, the memory epoch (Mem) was used as the baseline. The gray box denotes the post-saccadic epoch. (E and F) Same as (C)and& (D), ordered by modulation/tuning onset relative to target onset, starting 200 ms before target onset.

Additionally, to assess non-hemifield-specific spatial tuning, a permutation-based one-way ANOVA with factor 'target position' [David Stern (2023). randanova1 (https://www.mathworks.com/matlabcentral/fileexchange/44307-randanova1), MATLAB Central File Exchange. Retrieved January 16, 2023], as well as a permutation-based two-way ANOVA with factors 'target eccentricity' and 'target direction' [David Stern (2023). randanova2 (https://www.mathworks.com/matlabcentral/fileexchange/44308-randanova2), MATLAB Central File Exchange. Retrieved January 16, 2023] were used.

Response modulation

To assess task-related activity irrespectively of spatial tuning, enhancement or suppression of neuronal activity for each unit in each epoch was determined in two or three steps. We refer to the enhancement or the suppression of neuronal firing as the "response modulation" without implying any relation to "driving" vs. "modulatory" inputs to the pulvinar. Firstly, we performed the same permutation test as for hemifield tuning above, to compare firing rates in the tested epoch against a respective preceding baseline epoch, across all instructed trials. For cue onset and memory epochs (as well as 'cue onset 2' and 'pre-saccadic 2' for comparison with visually-guided task), the fixation hold epoch served as baseline. The memory epoch served as baseline for subsequent saccade-related epochs. Secondly, the *P*-values derived from permutation tests were corrected for multiple comparison across five epochs using the FDR procedure. Enhancement or suppression was reported if firing rates showed significant difference to the respective baseline. Thirdly, for units that showed hemifield preference but no enhancement or suppression across all instructed trials, we performed the permutation test *separately* for contralateral and ipsilateral trials, FDR-corrected for multiple comparison across 10 *P*-values (contra- and ipsilateral × five epochs) and reported enhancement or suppression if at least one of the hemifields showed significant difference from baseline ($q(FDR)<0.05$). In rare cases where the response in one hemifield was significantly enhanced while the other was significantly suppressed, the response for the hemifield with the largest absolute firing rate difference to the baseline was reported.

Units that showed enhancement or suppression in both cue onset and post-saccadic epochs were classified as visual-saccadic units, whereas units that only showed enhancement or suppression in one of the two epochs were classified as visual (only enhancement or suppression in cue onset epoch) and saccade-related (only enhancement or suppression in post-saccadic epoch). Visual-saccadic index (VSI) was defined independently for ipsilateral and contralateral trials as $(S - V)/(S + V)$, where S is the absolute average firing rate change in post-saccadic epoch relative to the memory epoch, and V is the absolute average firing rate change in cue onset epoch relative to fixation hold (Lawrence et al. 2005).

In addition to the VSI described above, we also used classical visuomotor categories derived using enhancement or suppression in cue onset and motor-related pre-saccadic (as opposed to post-saccadic) epochs relative to fixation hold. This was done to compare the results to previously used visuomotor categorizations (Bruce and Goldberg 1985; Wyder et al. 2003).

Peri-stimulus time histograms

To calculate population Peri-stimulus time histograms (PSTHs), spike density functions of each trial were derived by convolution of the discrete spike arrival times with a Gaussian kernel (SD 20 ms), binned at 10 ms and normalized by dividing by the average firing rate (across all trials) in the fixation hold epoch. Average responses for each unit were then derived by averaging the normalized spike density across all trials for the respective condition. Means and SE of these baseline-corrected and averaged spike densities across units of a given sub-population were calculated to display population responses.

Response modulation and tuning timecourse analysis

To evaluate the timecourse of response modulation and spatial tuning for each unit, spike density functions with a Gaussian kernel SD 10 ms, binned at 10 ms, were calculated. For the three alignments (to cue onset, saccade onset, and target onset), spike densities for each bin were compared with the average firing rate in the respective trial baseline epoch (fixation hold for cue alignment and memory for saccade and target alignment) using *paired* cluster-based permutation tests with 10,000 permutations, $P < 0.05$ cluster-forming threshold and $P < 0.05$ cluster critical value (Maris and Oostenveld 2007) [Edden M. Gerber (2023). permutest (https://www.mathworks.com/matlabcentral/fileexchange/71737-permutest), MATLAB Central File Exchange. Retrieved January 16, 2023] across all trials to evaluate bin-by-bin modulation. Significant positive clusters were reported as enhancement and significant negative clusters as suppression. Similarly, for each bin, the spike densities of contralateral trials and ipsilateral trials were compared using *unpaired* cluster-based permutation tests, using the same function. Significantly higher spike density for contralateral trials was reported as contralateral preference and significantly higher spike density for ipsilateral trials as ipsilateral preference. Additionally, we counted the number of units which showed significant modulation in each bin and calculated the time in which most units were modulated. Based on the finding that most units showed enhancement and contralateral preference at 110 ms after cue onset (cf. Fig. 2A,B), the cue onset epoch was selected as 50 ms before to 50 ms after that maximum.

Response fields and interactions between hemifields

To estimate the center and the extent of visual and post-saccadic response fields (RFs), we fitted 2D Gaussian distributions on the response strength averages per target position, weighted by inverse of response variation per position, in cue onset (Cue) and post-saccadic (Post) epoch. Response strengths were calculated relative to the respective baseline, by subtracting firing rates in fixation hold (Fhol) for visual cue responses and firing rates in the memory epoch (Mem) for post-saccadic responses. This analysis was only performed on units that showed enhancement or suppression for at least one hemifield in the respective epoch. The fitting of RFs was performed in two steps: first, one Gaussian RF zone was fitted, allowing either a positive or a negative peak. The second Gaussian RF zone was fitted allowing only the opposite sign of the peak, and not allowing overlap with the first zone. Significant fits were reported if the absolute residuals of at least one of the RF zones were significantly smaller than the absolute residuals to the zero plane fit ($P < 0.05$, one-tailed unpaired *t*-test). An RF with two zones was reported if absolute residuals were significantly smaller when using both RF zone fits than when only using the first RF zone fit ($P < 0.05$, one-tailed unpaired *t*-test).

Six fitting parameters for each Gaussian response zone were determined using an iterative least squares method (400 iterations), allowing elliptic response zones with peaks (or troughs) at the center. The fitting parameters were as follows: (1) the response strength in the center of zone, (2) horizontal and (3) vertical location of the center of the response zone, (4 and 5) standard deviations describing semi-minor and semi-major axes, and (6) an angle of rotation of these axes. Importantly, the response zone centers were always kept within the dimensions of the target array (–24° to +24° horizontally and (–8° to +8° vertically). The response strength was bounded by –150 and 150% of the original maximum response strength, standard deviations were bounded by 1.5° (a quarter of the maximum horizontal target distance) and 12° (a quarter of the horizontal extend of the target array), and the rotation was unbounded.

The size of each elliptic zone was defined by two standard deviations in each direction (semi-minor and semi-major axes). A radius r approximating response zone size was calculated by taking the square root of the product of the two axes of the elliptic zones. This way, πr^2, always matches with the area covered by the elliptic response zone. Response zone size is reported as diameter, $2r$. For units with one response zone, RF size was defined equal to response zone size. For units with two response zones, we reported the size of the larger response zone.

To assess potential interactions between hemifields, we compared firing rates in instructed and choice trials in the preferred hemifield. To avoid introducing a systematic instructed > choice firing rate bias, the preferred hemifield was determined by 100 iterations of bootstrapping instructed firing rates. In each iteration, 50% of instructed trials were used to determine the preferred hemifield, while the other 50% were used to compute the instructed response. Average firing rates were computed by averaging across all bootstrap iterations.

Choice selectivity

To see if information about the upcoming target selection could be derived from spiking activity, we correlated instructed and choice firing rate differences between contralateral and ipsilateral trials using Pearson's correlation. For this analysis, units were considered only if at least 24 choice trials to each hemifield were recorded. The contralaterality index in instructed and choice trials was calculated as CI = (firing rate $_{contra}$ – firing rate $_{ipsi}$/ (firing rate $_{contra}$ + firing rate $_{ipsi}$). For comparing the absolute strength of spatial selectivity in instructed vs. choice trials, we subtracted the absolute CI_{instr} and CI_{choice} values and tested the significance of difference using paired Wilcoxon's signed rank test.

Results

Response timing and tuning in memory-guided saccade task

We recorded dorsal pulvinar spiking activity in two monkeys performing a memory-guided saccade task. Trials always started with initial fixation in the center of the screen followed by a cue or two cues, memory delay and saccade to one out of 12 peripheral instructed or chosen locations (Fig. 1A and Materials and Methods).

The activity of one example unit and the eye traces for two cue/target positions are shown in Fig. 1(B). This unit shows an enhanced visual response after the cue presentation at contralateral positions as well as a contralateral post-saccadic response which cannot be attributed to a target-related visual response because it occurs before the onset of the visual target (Tar onset).

To evaluate how population activity of all 322 units selected for the analysis developed over trial time (and to validate the timing of analysis epochs), we estimated significant enhancement or suppression as well as hemifield preference for each unit in 10 ms bins (Fig. 2, see also Materials and Methods). In Fig. 2(A, B), top rows units are ordered by the start of significant modulation or spatial tuning after cue onset (or before the cue onset if the modulation appeared prior to the cue but overlapped with the cue). The fixation hold epoch was used as baseline. The modulation preceding the cue onset in few units could be due to monkeys anticipating the cue after a fixed fixation hold period. The underlying activity was either aligned to cue onset (left) or saccade onset (right). This analysis showed a time-locked enhancement shortly after the cue onset and a predominance of suppression during the memory period (Fig. 2A) combined with contralateral cue preference shortly after the cue onset and an overall lack of spatial preference during the memory epoch (Fig. 2B). For quantification, we plotted the number of units showing significance in each bin to identify periods of strong population response (Fig. 2A, B, bottom rows). While enhancement and contralateral preference typically started at around 50 ms after cue onset, the timing of suppression and ipsilateral preference was more dispersed. Enhancement was most common at 120 ms after cue onset, close to the time bin where most units showed contralateral preference (110 ms after cue onset).

In Fig. 2(C, D), units are ordered by the start of modulation/tuning in the period from 200 ms before saccade onset. Because of the frequent differences in firing rate between initial fixation and memory periods, here (and in Fig. 2E) we used the memory epoch as baseline for the modulation around the saccade. We observed predominantly post-saccadic enhancement (Fig. 2C) with a bias to the contralateral hemifield (Fig. 2D). Pre- and peri-saccadic modulation was rare compared with post-saccadic modulation, and enhancement was widely spread in the post-saccadic period, reaching maximum at 220 ms after saccade onset (or 170 ms after saccade end). The suppression peaked earlier, at 135 ms after saccade onset (or 85 ms after saccade end). The analysis of potential effects related to screen background luminance suggests that at least in a sizable fraction of units spatially-tuned post-saccadic activity is not due to stimulation by the screen (Supplementary Table S2), although activation by rapid retinal image shifts cannot be ruled out, especially in the non-tuned responses.

To evaluate the impact of the visual reappearance of the confirmation target, in Fig. 2(E, F), the activity was aligned to target onset, and units were ordered by the start of significant modulation in the period beginning 200 ms before the target onset. Importantly, most units showed enhancement or suppression (Fig. 2E) or hemifield preferences (Fig. 2F) before the target reappearance. This suggests that post-saccadic responses are primarily not attributable to direct visual stimulation by the (para)foveal target reappearance. The fraction of units that showed enhancement after the target onset reached the maximum at 70 ms (Fig. 2E), earlier then for cue responses (120 ms). This might indicate a difference in timing of visual responses for peripheral (cue) and central (target) stimuli.

Figure 3 shows the summary of response modulation and hemifield preference in five task-relevant epochs in instructed trials. If there was no significant hemifield preference, we tested one-way permutation-based ANOVA across 12 target positions, to account for units with upper/lower visual field selectivity or idiosyncratic tuning profile. The majority of units (76%) showed task-related enhancement or suppression in at least one of the analyzed epochs, and an additional 6% showed hemifield tuning in at least one epoch (all tests corrected for multiple comparisons, see Materials and Methods). To summarize the main patterns: (1) the contralateral hemifield preference was more common than the ipsilateral preference in the cue onset epoch (16% vs. 4%, $P < 0.001$, Fisher's exact test), and majority of units with the contralateral cue preference (37/53) showed the enhancement. (2) The number of units preferring contralateral or ipsilateral hemifield became equalized in subsequent epochs, and hemifield preference was less frequent in memory (11%), pre-saccadic (11%), and peri-saccadic epoch (13%) as compared with the post-saccadic epoch (24%) (all $P < 0.0025$). (3) Enhancement was more common than suppression during the cue period (25% vs. 10%, $P = 0.0024$), the opposite was true in the memory

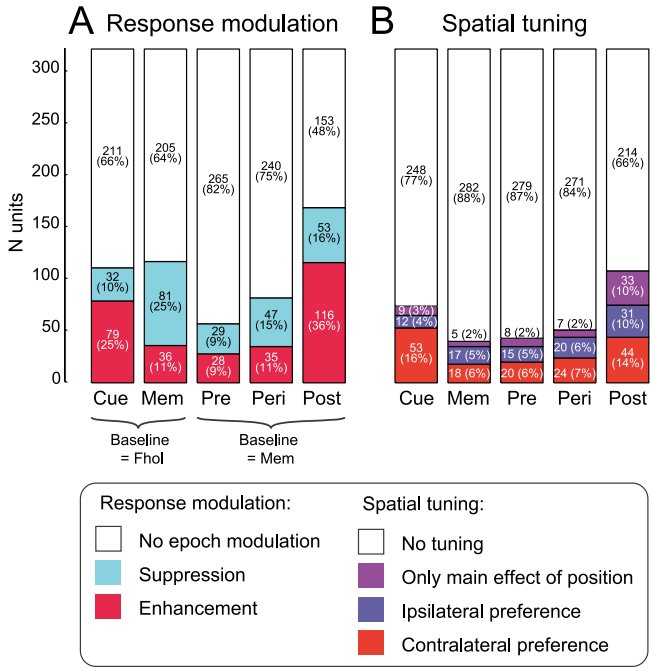

Fig. 3. Spatial tuning and response modulation per epoch. Spatial tuning and response modulation of all 322 units recorded during the memory-guided saccade task. The analyzed epochs are cue onset (Cue), memory (Mem), pre-saccadic (Pre), Peri-saccadic (Peri), and Post-saccadic (Post). (A) Total number of units (and percentages) showing response modulation relative to the respective baseline, for each analyzed epoch: no modulation (white), suppression (blue), enhancement (red). (B) Number of units (and percentages) that were not tuned (white), did not prefer either hemifield but showed a main effect of position in a one-way permutation based ANOVA (purple), preferred ipsilateral hemifield (blue), preferred contralateral hemifield (orange). The patterns of response modulation and tuning were largely comparable across the two animals. The most noticeable difference between monkeys was that monkey C showed stronger contralateral cue preference (N=41) compared with ipsilateral cue preference (N=3) than monkey L (N=12 and 9, respectively). See Supplementary Fig. S1 for the relationship between response modulation and spatial tuning in each epoch.

period (11% vs. 25%, P = 0.005), and both effects were balanced before and during the saccade (9% vs. 9% in pre-saccadic and 11% vs. 15% in peri-saccadic epochs). After the saccade, activity was typically enhanced (36% enhancement vs. 16% suppression in the post-saccadic epoch, $P < 0.001$). For details of how enhancement/suppression and spatial tuning patterns interrelate, please refer to Supplementary Fig. S1.

Cue and saccade RF properties

To further characterize spatial selectivity in the two epochs with most response modulation, we compared visual and post-saccadic RFs. We fitted Gaussian RF zones for each unit that showed significant enhancement or suppression in the respective epoch (N=111 visual and N=169 post-saccadic responses, Fig. 4A, B), allowing one enhanced and/or one suppressed zone (Materials and Methods). Figure 4(C) shows a summary of RF zones for both epochs. Visual RFs were mostly fitted by contralateral enhancement (N=51, 54% of all significant fits), the centers of enhanced post-saccadic RF zones were distributed over both hemifields. Units showing visual enhancement were often fitted with elliptical RFs (68 out of 79, 86%); less numerous units showing visual suppression also often had elliptical RFs (25 out of 32, 78%). Conversely, post-saccadic enhancement was fitted less often (84/116, 72%) than post-saccadic suppression (49/53, 92%), indicating that post-saccadic enhancement was less topographically consistent (P = 0.013; Fisher's exact test). The visual RFs were less extensive than post-saccadic RFs (mean ± SD 28.1 ± 9.1° and 33.3 ± 11.9° respectively; $P < 0.001$, unpaired t-test).

Given that most RFs were large, and some were bilateral with centers near the fovea, we next assessed the relative impact of the direction of a target relative to central fixation vs. its absolute eccentricity. To this end, we performed a direction × absolute eccentricity two-way permutation ANOVA on firing rates in the cue and post-saccadic epoch (Supplementary Fig. S2). Out of the 107 units showing at least one of the two main effects or an interaction in the cue epoch, most (57) units showed only the main effect of direction, 35 units showed some combination of direction and eccentricity effects, and only 15 units showed exclusively the main effect of eccentricity. Likewise, in the post-saccadic epoch out of 175 units with at least one main effect or interaction most (70) units showed only the main effect of direction, but a considerable number (34 units) showed only the main effect of eccentricity. This further illustrates that the non-directional eccentricity dependence, while more frequent in post-saccadic responses compared with visual responses, was a not a common pattern.

To assess potential interactions between hemifields, we asked if the visual stimulus in the opposite hemifield affects the response to the stimulus in the preferred hemifield. Across units with significant cue enhancement, on average there was no difference between response amplitudes in unilateral vs. bilateral trials (Supplementary Fig. S3). But in line with our expectations, the horizontal RF size (the projection of the fitted RF to the horizontal axis) was larger for the units showing significant bilateral > unilateral response (inter-hemifield summation, six units, 21.2±3.3°) than for the units showing unilateral > bilateral response (inter-hemifield suppression; eight units, 12.7±6.7°, P = 0.015, unpaired t-test). Thus, while most units were not affected by the stimulus outside of the preferred hemifield, few units with smaller RFs showed inter-hemifield suppression, and few units with larger RF showed summation across the two hemifields.

Response pattern categorization

To characterize the firing patterns across the sample while taking into account relative predominance of cue and post-saccadic responses (as compared with less frequent pre-saccadic or peri-saccadic responses), we defined three response categories based on the response modulation (enhancement or suppression) during the cue onset and post-saccadic epochs. Visual (V) neurons were defined by statistically-significant enhancement or suppression during cue onset, but no modulation during the post-saccadic epoch, saccade-related (S) neurons by enhancement or suppression in the post-saccadic epoch, but not during cue onset, and visual-saccadic (VS) neurons—by enhancement or suppression in both epochs. Figure 5(A)–(C) shows two example units for each of these three categories, one example with enhancement during the respective epoch(s) on the left, and suppression on the right. The diversity of the response patterns is further illustrated by example units that showed enhancement or suppression during the memory epoch (Fig. 5D).

The localization of units categorized as V (N=39), S (N=97), or VS (N=72) neurons revealed no systematic distribution of the recording sites within the medial dorsal pulvinar (Fig. 6A). To further confirm the plausibility of this categorization, we computed a VSI

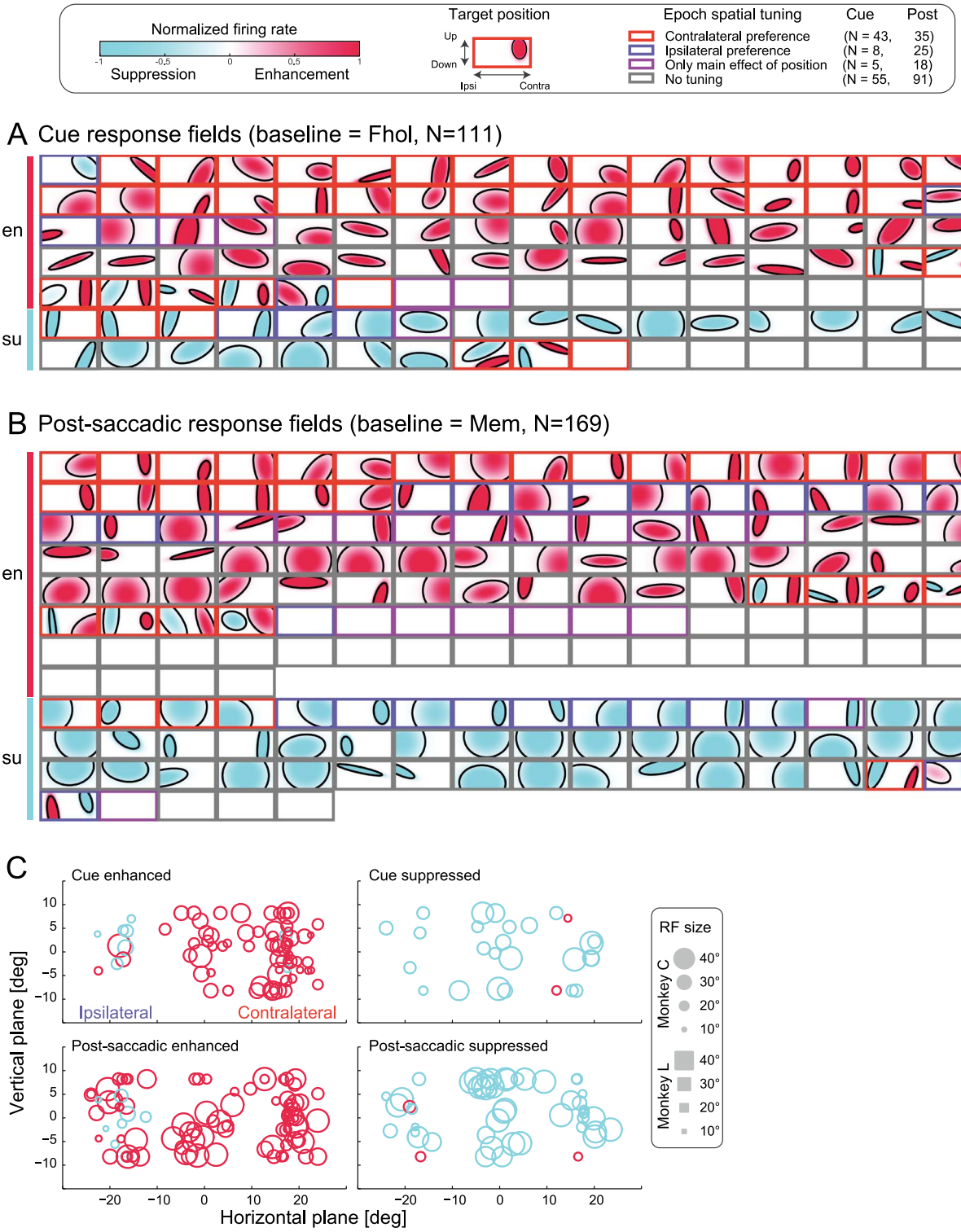

Fig. 4. Visual and post-saccadic RFs. (A) Visual RFs for units that showed enhancement (en) or suppression (su) during cue onset. Each subplot represents one unit. Response fields were allowed to have two zones, one enhanced (red) and one suppressed (cyan) relative to the respective baseline, see Materials and Methods. Only significant zones are plotted; empty subplots indicate no significant explanation of variance by the fitted response field. Firing rates are normalized to the maximum absolute response strength. The color of the frame for each subplot indicates the spatial tuning of the respective unit (significant unpaired *t*-test on contralateral trials versus ipsilateral trials and/or an permutation ANOVA effect of target position): contralateral preference (orange), ipsilateral preference (blue), only an ANOVA effect of target position (purple), or no spatial tuning (grey). The number of units showing enhancement or suppression in at least one hemifield and the respective tuning (contralateral preference, ipsilateral preference, main effect of ANOVA only, no tuning) is shown in the legend for the cue epoch (left number) and the post-saccadic epoch (right number). Note that units with an ipsilateral suppressed RF zone are expected to show contralateral preference according to our definition of hemifield preference (preferred hemifield is the hemifield with higher firing rate), and vice versa. (B) Same as A, for post-saccadic RFs. (C) Summary of all cue (top) and post-saccadic (bottom) response field zones, separately for enhanced and suppressed units. Each symbol represents one zone, circles for monkey C and squares for monkey L. The location and size of the symbols depicts the center and the size of the response field zone, and the colors indicate enhancement (red) or suppression (cyan).

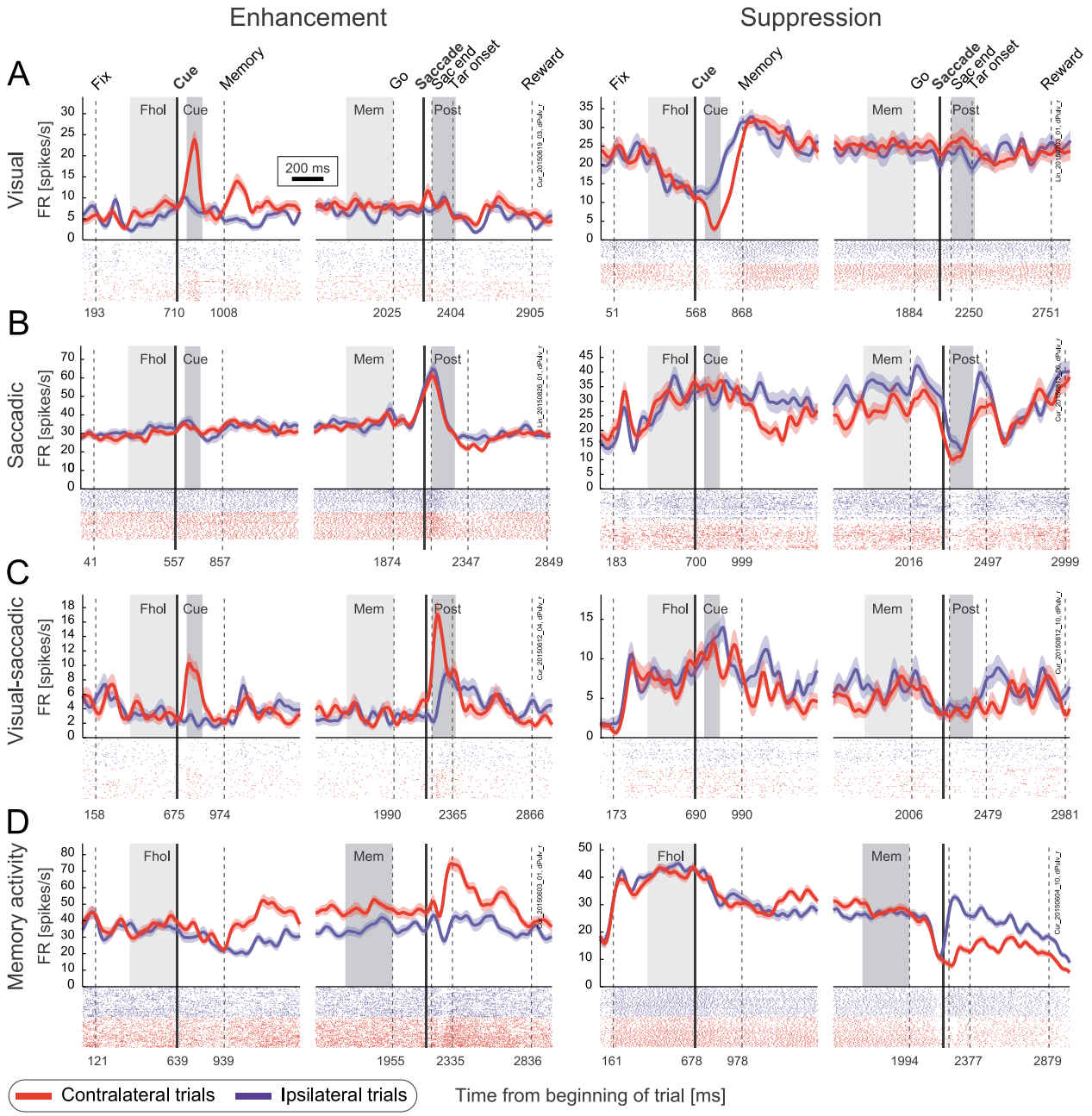

Fig. 5. Diversity of task-related activity: example units. Raster plots and spike density functions for contralateral (orange) and ipsilateral (blue) trials. Vertical lines indicate the average onset of events: the monkey acquiring fixation (Fix), the cue onset, the cue offset and beginning of the memory period, the offset of the central fixation point (Go), the saccade onset, the monkey acquiring the invisible target location (Sac end), the onset of the visible peripheral target, and the end of the trial (Reward). Discontinuous traces indicate two different alignments to cue onset and saccade onset (continuous vertical lines). Light gray (baseline epochs) and gray boxes mark relevant analyzed epochs: fixation hold (Fix), cue onset (Cue), memory (Mem), and post-saccadic (Post). Examples for four different categories are shown. (A) Visual units (enhancement or suppression in Cue relative to Fhol; (B) saccade-related units (enhancement or suppression in Post relative to Mem); (C) visual-saccadic units (enhancement or suppression in both Cue and Post); (D) units with memory activity (left: hemifield preference in Mem, right: suppression in Mem compared with Fix).

(ranging from –1 for purely visual to 1 for purely saccade-related response) for each unit independently for the ipsilateral and the contralateral hemifield (see Materials and Methods) and tested if the mean VSIs in each group were significantly different from zero. As expected, VSIs of visual units were significantly negative and VSIs of saccade-related units were significantly positive, see Fig. 6(B) ($P < 0.001$ for all four tests, one sample t-test). Interestingly, VSIs of visual-saccadic units were significantly positive for the ipsilateral hemifield ($P < 0.01$), while for the contralateral hemifield VSIs of visual-saccadic units were not different from zero ($P = 0.28$). This indicates stronger saccade-related responses for ipsilateral saccades as compared with visual responses to ipsilateral stimuli in visual-saccadic units. The categories however overlapped and there were no separate modes in VSI distributions, indicating a continuum of visual and saccade-related properties. We retain these categories for subsequent analyses as a tractable approach to the heterogeneity of response patterns, but do not imply separable groups.

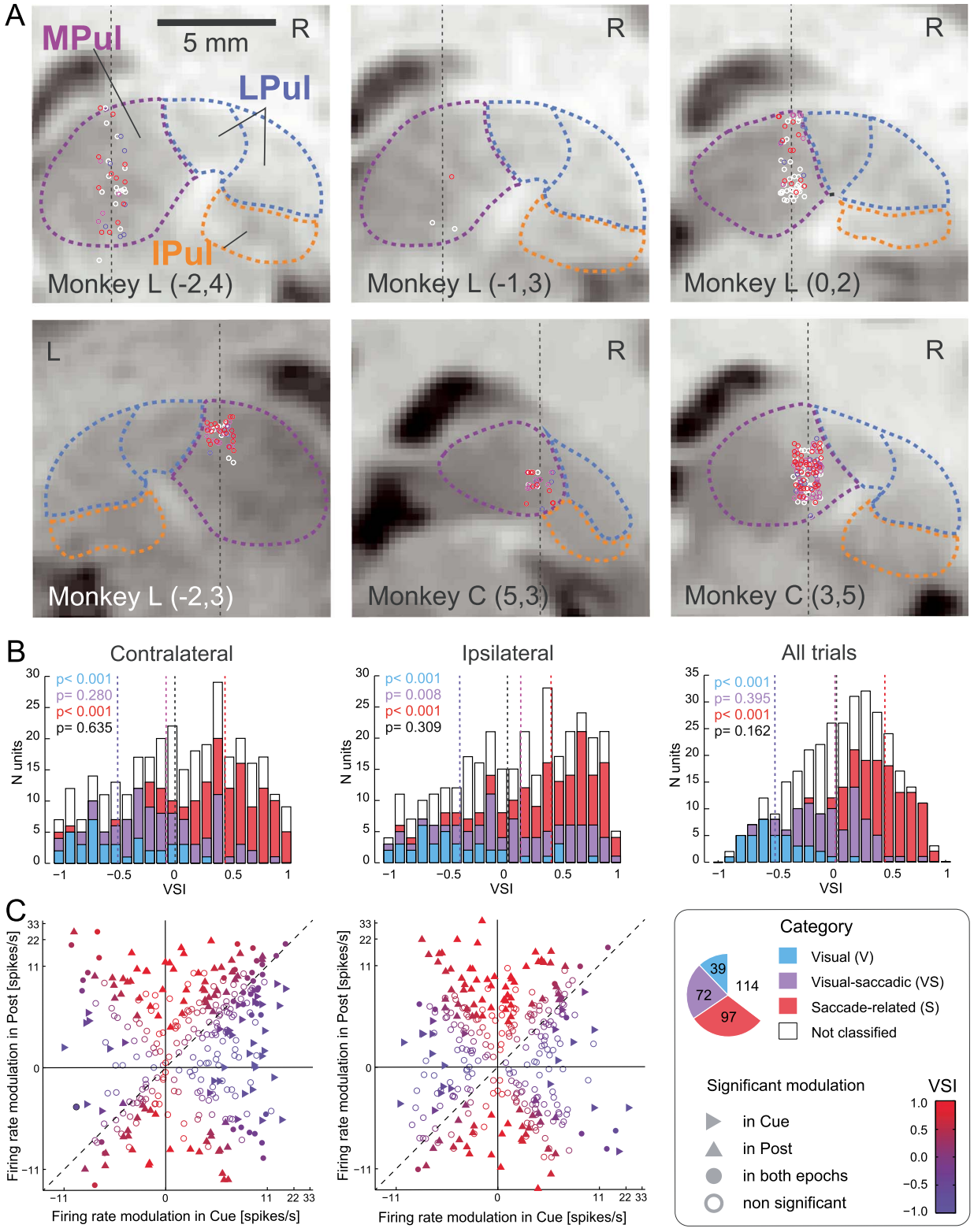

Fig. 6. Visual-saccadic categories. (A) Localization of recorded units (N=322) in chamber-normal coronal sections in each monkey (L and C, labels on the bottom) and specific grid locations (x, y in parentheses). Locations were jittered along the horizontal axis for better visualization. The black dotted lines indicate the electrode tracks and mark the actual horizontal location of recorded neurons. Colors indicate the category of the unit; blue for V, purple for VS and red for S units. Units that did not fall within any of these categories are shown as white circles. Pulvinar nuclei outlines (MPul/LPul/IPul—medial/lateral/inferior pulvinar) were adapted from the NeuroMaps atlas (Rohlfing et al. 2012), exported via Scalable Brain Atlas, https://scalablebrainatlas.incf.org/macaque/DB09, https://scalablebrainatlas.incf.org/services/rgbslice.php, (Bakker et al. 2015), and LPul was further subdivided to dorsal (PLdm) and ventral (PLvl) parts. B: Histograms of VSIs computed for contralateral trials (left), ipsilateral trials (middle), or all trials (right). Colors denote the category. P-values indicate results of one sample t-tests against zero. (C) Scatter plots comparing the firing rate modulation in Cue and Post-saccadic epochs, for contralateral trials (left) and ipsilateral trials (right). Colors indicate the respective VSI (legend inset on the right). For better visualization, firing rate modulation was plotted on a logarithmic scale. The pie plot on the right shows the total number of units for each of the categories.

To further test if specific sub-groups would be evident across the entire population, we plotted post-saccadic modulation versus cue modulation across the entire population (Fig. 6C). Besides a more frequent occurrence of units in the upper right quadrant with enhancement in both the cue onset and the post-saccadic epochs in contralateral trials ($P = 0.0007$, χ^2=16.9, 38 units significant in both epochs), the units were distributed fairly uniformly, further indicating a continuum of responses.

Population PSTHs for the three categories show enhancement for contralateral cues in visual and visual-saccadic units, and post-saccadic enhancement with only weak spatial preference in visual-saccadic and saccade-related units (Fig. 7A, top). Visual neurons show only a very small bump after a saccade but respond later to a confirmation target onset, saccade-related neurons respond to the saccade, and visual-saccadic neurons respond to both events. A more detailed picture can be gained by further separating these three categories based on enhancement or suppression either in the cue onset or the post-saccadic epochs, and analyzing the preferred target position for each unit (the position that exhibited the strongest response modulation in the respective epoch, Fig. 7A, bottom). Two observations can be made. First, visual-saccadic units showing suppression in the cue epoch relative to fixation hold are typically also suppressed throughout the entire trial, including memory delay (although the visual conditions are identical in the fixation hold and memory periods). Second, the net enhancement of visual-saccadic and saccade-related units in the post-saccadic epoch is a result of unequal proportions of enhanced and suppressed units (*N*=52 and 20, 72 and 28% of visual-saccadic units; *N*=64 and 33, 66 and 34% of saccade-related units).

To delineate the contribution of units with different spatial preferences and enhancement or suppression, without dilution caused by averaging the opposing patterns, we defined subpopulations in each category based on the conjunction of tuning and response modulation (Supplementary Table S3 and Supplementary Fig. S4). Among other insights, this analysis showed the following: (1) the weak overall post-saccadic contralateral preference was due to a larger proportion of contralaterally-tuned than ipsilaterally-tuned units, on top of a large fraction of units without tuning; (2) most units with clear post-saccadic suppression were not spatially-tuned; and (3) contralaterally-tuned saccade-related group also exhibited pre- and peri-saccadic ramping.

Since we were also interested in characterizing pre-saccadic activity that might reflect motor preparation, Fig. 7(B) illustrates the same analysis based on the categorization using response modulation in the *pre*-saccadic epoch (Materials and Methods). compared with the post-saccadic responses, fewer units showed pre-saccadic enhancement or suppression. Importantly, the post-saccadic enhancement is still evident in the population responses of all three categories, while enhancement and suppression as well as spatial preference in the pre-saccadic epoch balances out across the sample (Fig. 7B, top), due to opposing contributions of enhanced and suppressed units (Fig. 7B, bottom). This further supports a classification based on post-saccadic responses.

To explore the relationship between different components of saccade-related responses (putatively motor-related pre- and peri-saccadic activity vs. post-saccadic activity), we made pairwise comparisons across these epochs (Supplementary Fig. S5). This analysis showed significant correlation of response modulation in all three pairs (all $P < 0.001$; but weaker $R = 0.27$ correlation between pre- vs. post-saccadic epochs compared with the other two pairs, $R = 0.52$ or 0.51). In pre- vs. peri-saccadic epoch, the activity was mainly either congruent (suppression or enhancement in both epochs), or only present in the peri-saccadic epoch. However, the fraction of units with congruent peri- vs. post-saccadic responses, and especially pre- vs. post-saccadic responses was much smaller than the fraction of units with only post-saccadic activity. Thus, while some units show a consistent pattern of activity before, during and after the saccade, there is a progression from few units responding only before the saccade, to more units responding only during the saccade, to many more units responding during and after or only after the saccade.

Delay period activity in relation to pre-/peri-saccadic activity

Due to the strong bidirectional connectivity between dorsal pulvinar and posterior parietal cortex (PPC), in particular area LIP (Hardy and Lynch 1992; Gutierrez et al. 2000) as well as the suggested role of pulvinar in guiding goal-directed actions (Grieve et al. 2000; Wilke et al. 2010b), we predicted that some dPul neurons show delay period activity smoothly merging into pre-/peri-saccadic responses—a hallmark of canonical PPC responses (Barash et al. 1991a; Premereur et al. 2011). As reported previously (Dominguez-Vargas et al. 2017), population averages for units that showed either enhancement or suppression in the peri-saccadic epoch as compared with fixation hold appeared to show ramping up (*N*=41) or ramping down (*N*=82), reaching the respective maximum or minimum during saccade execution (Fig. 8A, B). Normalizing these two subsets using division by average firing rate in fixation hold rather than subtracting inter-trial-interval activity confirmed that impression (Fig. 8C, D). However, here we demonstrate that the continuously ramping up delay period activity culminating at the saccade is largely a result of combining different subpopulations. First, subpopulations showing peri-saccadic enhancement (*N*=35) or suppression (*N*=47) relative to memory did not exhibit ramping or persistent delay period activity (Fig. 8E, F). Second, subpopulations showing enhancement or suppression in memory relative to fixation hold (*N*=36 and 81, respectively) did not exhibit pronounced peri-saccadic responses (Fig. 8G, H). In fact, very little overlap between these subpopulations was found: only three units showed significant enhancement in memory relative to fixation hold and in peri-saccadic epoch relative to memory, and 16 units showed suppression in both epochs. Besides these few consistently ramping up/down units, subpopulations shown in Fig. 8(A, C) and (B, D) combine units that showed enhancement or suppression during memory (relative to fixation) with units that showed enhancement or suppression during the peri-saccadic epoch (relative to memory). Interestingly, the enhanced memory delay firing stayed at the same level throughout the entire period (Fig. 8G), whereas activity was decreasing gradually in the subpopulation showing suppression in the memory epoch (Fig. 8H).

In studies of parietal cortex, neurons showing enhanced firing to visual cues are often selected online or offline for further analyses of delay period activity (Colby et al. 1996; Ipata et al. 2006; Chen et al. 2016); see also a recent study in the pulvinar (Fiebelkorn et al. 2019). Our sample was acquired without taking into account any response properties online; across the subset of 79 units that exhibited enhanced cue response in the offline analysis, the curves for the preferred and non-preferred target positions largely overlapped during the delay. Likewise, across the entire sample the curves for contralateral and ipsilateral positions largely overlapped in the late memory delay (Supplementary Fig. S6). Figure 8(I, J) shows specific subpopulations that were significantly tuned for contralateral or ipsilateral space in the memory delay. The contralaterally- and

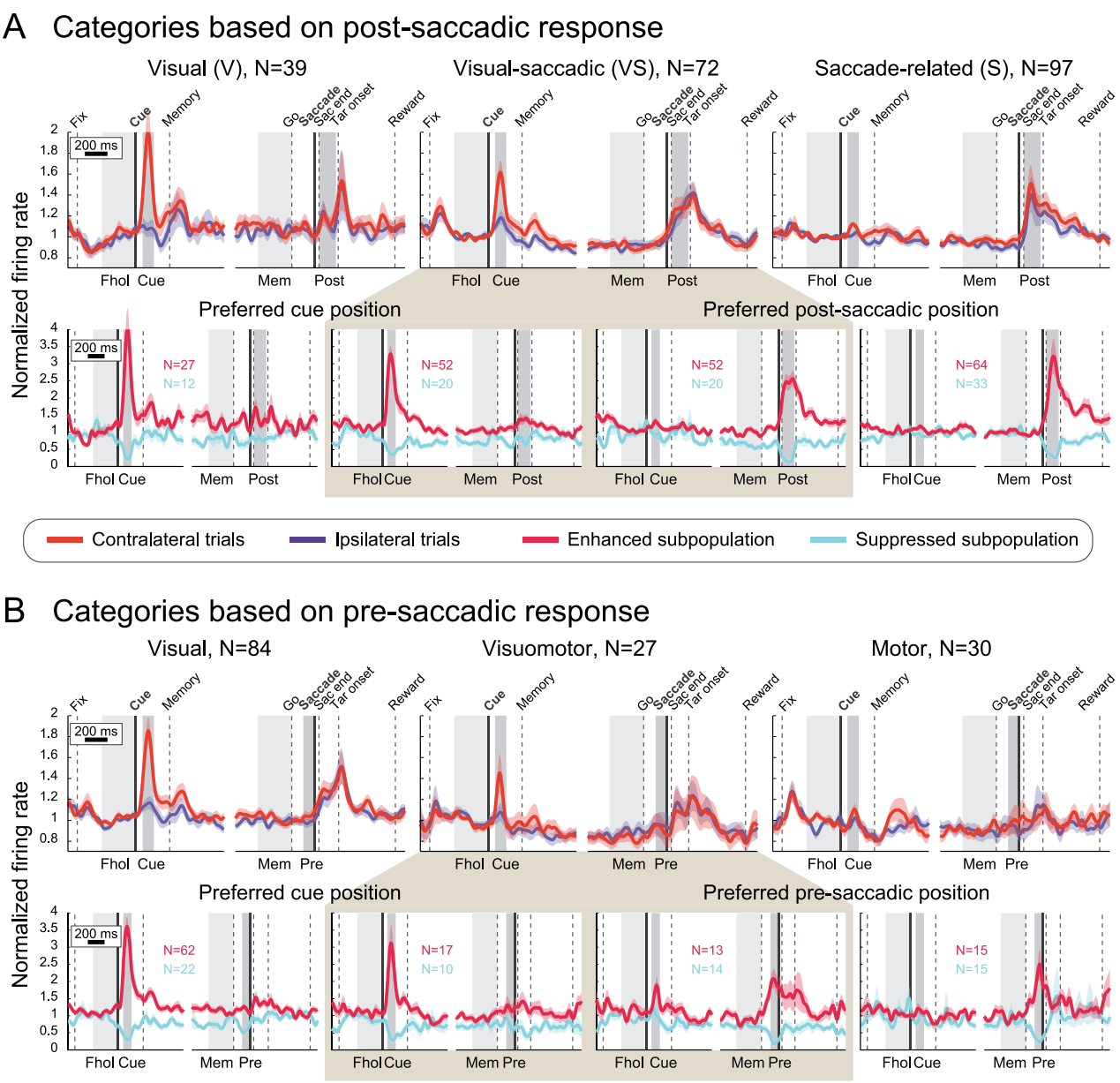

Fig. 7. Population responses of the three categories. (A) Visual, saccade-related and visual-saccadic units. Top: population responses for contralateral (orange) and ipsilateral (blue) trials. Bottom: subpopulations showing enhancement (red) or suppression (cyan) during either cue or post-saccadic epoch. For each unit, only the response for the most modulated cue/target position (location with the largest absolute firing rate difference from baseline) in the respective epoch was taken. (B) Same as (A), for the categorization based on pre-saccadic response (Pre epoch) instead of post-saccadic response.

ipsilaterally-tuned units differed in terms of response pattern: the contralaterally-tuned group showed a congruent contralateral cue tuning (but no pre-/peri-saccadic enhancement), while the ipsilaterally-tuned group showed incongruent contralateral cue tuning as well as peri-saccadic suppression in ipsilateral trials.

These findings have two important implications. First, only a small minority of units showed "classical" spatially-tuned cue-delay-saccade enhancement, and the units that exhibited sustained delay activity showed no ramping toward the saccade, constraining the role of individual dPul neurons in prospective motor planning. Secondly, more units showed delay period suppression and *ramping down* than enhancement, and most of these units showed cue suppression or no cue response (61 out of 81 units with memory delay suppression), suggesting putative inhibitory projections from a subset of pulvinar units to the frontoparietal circuitry, or conversely a cortically-driven inhibition on the pulvinar.

Comparison of memory-guided and visually-guided saccade tasks

To evaluate how the presence of a visible saccade target and the immediate response context might affect pre-saccadic activity as compared with memory-guided saccade, in a subset of sessions we also recorded the same units while monkeys were performing a visually-guided saccade task. In the visually-guided task, monkeys had to perform a saccade immediately after the onset of the target(s) (Materials and Methods).

We compared the response modulation in the target onset/pre-saccadic epoch in the visually-guided task against two partly corresponding epochs in the memory-guided task: 'cue onset 2' that encompassed most visual responses, 40–140 ms after the

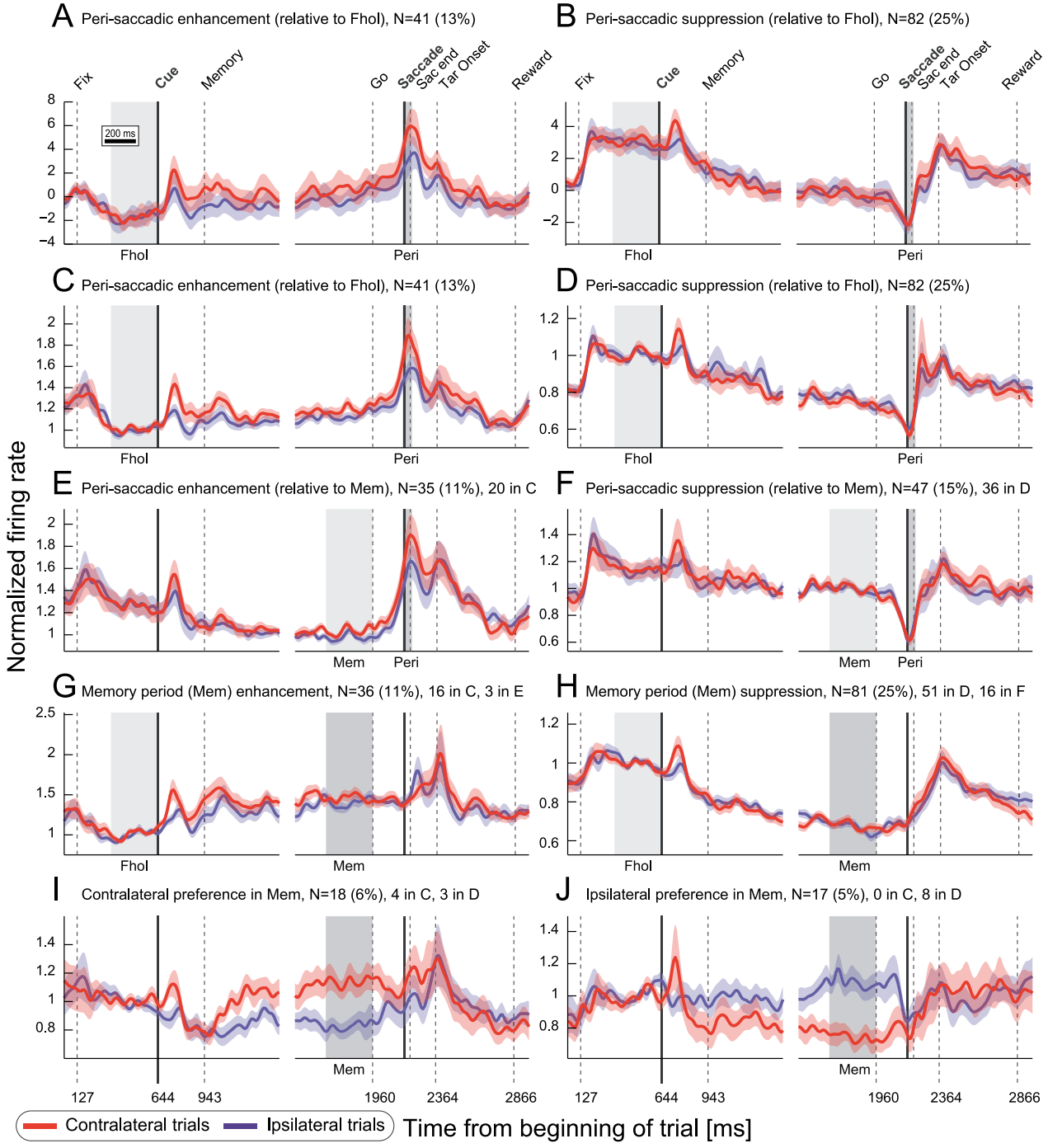

Fig. 8. Delay period and peri-saccadic activity. Population responses for contralateral (orange) and ipsilateral (blue) trials. Vertical lines mark events, colored areas—relevant epochs for population definition. (A) Average of units showing peri-saccadic enhancement relative to fixation hold epoch (FhoI), normalized by subtracting the average firing rate in inter-trial-interval epoch. (B) Same as (A), for units showing peri-saccadic suppression. (C) Average of units showing peri-saccadic enhancement relative to FhoI (same units as in A), normalized by dividing the spike density functions by the average firing rate in FhoI. (D) Same as (C) for units showing peri-saccadic suppression. (E) Average of units showing peri-saccadic enhancement relative to the memory epoch (Mem). (F) Same as (E) for units showing peri-saccadic suppression. (G) Average of units showing enhancement in Mem relative to FhoI. (H) Same as (G) for units showing suppression. (I) Average of units showing contralateral preference in Mem. (J) Same as (I) for units showing ipsilateral preference. Additional text on top of (E)–(J) shows number of units in the current panel overlapping with other indicated panels.

cue and 'pre-saccadic 2' that encompassed motor preparation signals, 130–30 ms before the memory saccade onset. These epochs differ slightly from the original cue (70–170 ms after cue onset) and pre-saccadic (100–10 ms before saccade onset) epochs, and were chosen to be comparable to the combined target onset/pre-saccadic epoch 40–140 ms after the target onset ('target-pre-sac') in the visually guided task—where this interval was chosen to not overlap with the saccade onset.

Response modulation was correlated across units in the two tasks, both when comparing 'target-pre-sac' response to either visual ('cue onset 2') or pre-saccadic responses ('pre-saccadic 2') ($P < 0.001$ for 'cue onset 2' for both hemifields, $P = 0.061$ for

Table 1. Saccade RTs and spatial target selection. *P*-values are from paired *t*-tests comparing session means.

	Hemifield	Instructed RT	Choice RT	*P*-value (instr. vs. choice RT)	% selected	*P*-value (selection left vs. right)
Monkey C	Left	209	204	0.004	58 ± 3	0.034
	Right	217	212	<0.001	42 ± 3	
Monkey L	Left	192	193	0.5	51 ± 5	0.889
	Right	188	185	<0.001	49 ± 5	

'pre-saccadic 2' ipsilateral, $P = 0.002$ for 'pre-saccadic 2' contralateral, Pearson's correlation). This indicated that both visual and motor preparatory signals contribute to response modulations in the visually-guided task. To assess if the response modulation in the visually-guided task can be explained by the sum of visual and motor preparation signals, we compared activity in the 'target-pre-sac' to the sum of 'cue onset 2' and 'pre-saccadic 2' responses. The 'target-pre-sac' response modulation was stronger than the sum of separate epochs, suggesting supralinear summation of visual and premotor activity ($P = 0.001$ for contralateral trials, $P < 0.001$ for ipsilateral trials; paired *t*-tests). This was particularly true for units showing enhancement in the visually-guided task (contralateral trials: $N=50$, $P < 0.001$; ipsilateral trials: $N=19$, $P = 0.004$; paired *t*-tests). Thus, the immediate response context of the visually-guided task enhanced pre-saccadic activity.

Spatial choice selectivity

So far we mostly considered single cue instructed trials (except in the section on RF properties). In another half of the trials, monkeys were presented with two cues equidistantly from the fixation point, and were free to select either of the two positions, for the same reward. There were six possible pairs of targets, and instructed and choice trials were randomly interleaved, discouraging monkeys to make selection before the cues were presented. It has been shown that in such conditions dPul inactivation biases the choice toward the ipsilesional hemifield (Wilke et al. 2013).

Target selection in choice trials was fairly balanced between the two hemifields in both monkeys (monkey C: 58/42%; monkey L: 51/49%) and RTs in choice trials were very similar to instructed trials. If anything, monkeys were slightly faster in choice trials (Table 1). The lack of additional delay in choice RTs suggests that monkeys made choices before the end of delay period.

To assess if spatial preference in dPul neurons during the delay period is linked to space-specific motor preparation and could therefore reflect the upcoming saccade decision, we analyzed choice trials in the subpopulations showing hemifield preference in instructed trials. On average, there was no hemifield preference in the delay period activity in choice trials, and the choice trial traces were situated between preferred and opposite hemifield instructed trials (Fig. 9A). This might indicate that in these units, the spatially-selective delay activity in instructed trials is not directly linked to prospective target selection and motor preparation, but to retrospective maintenance of information about the visual stimuli presented earlier in the trial, or attentional allocation.

Some units however showed a significant difference in firing rates prior to selection of the contralateral or ipsilateral target in choice trials, well before the saccade. The pertinent question is whether the spatial selectivity in choice trials is mostly congruent to the spatial selectivity in instructed trials, as would be expected from neurons participating in motor decision and prospective planning (Coe et al. 2002; Watanabe and Funahashi 2007; Klaes et al. 2011; Pastor-Bernier and Cisek 2011; Suriya-Arunroj and Gail 2019). Figure 9B shows four example units with different types of cue tuning: (i) with congruent hemifield preference in instructed and choice trials, (ii) only in instructed trials, (iii) only in choice trials, and (iv) no hemifield preference in either instructed and choice trials. To evaluate if pulvinar neurons encode the upcoming choice across the population, we compared hemifield preference between instructed and choice trials in each unit in five epochs (cue onset, memory, pre-saccadic, peri-saccadic, and post-saccadic epoch). Before the saccade (cue, memory, pre-saccadic epochs) there was no systematic congruency between tuning in instructed and choice trials (Fig. 9C). Very few units showed a significant *congruent* effect of the (selected) hemifield in both trial types (cue: three units, memory: 0 units, pre-saccadic: four units), and across all units, hemifield preferences (firing rate difference contra—ipsi) were not correlated (cue: $P = 0.695$, memory: $P = 0.982$, pre-saccadic: $P = 0.762$, Pearson's correlation; the same result holds true for only those units that were tuned in the instructed trials). Furthermore, the strength of cue spatial preference (defined as the absolute contralaterality index, see Materials and Methods) was higher in instructed than in choice trials (instructed minus choice index difference 0.06 for all units, $P < 0.001$, Wilcoxon's signed rank test, and 0.28 for units tuned in instructed and/or choice trials, $P < 0.001$). As a control analysis, hemifield preferences were highly correlated between instructed and choice trials in peri- and post-saccadic epochs ($P < 0.001$, Pearson's correlation)—an expected result, given that the movements to the same target were similar in instructed and choice trials.

Because the choice selectivity could potentially be "washed out" by including multi-units, we also performed the same analysis on single units only ($N=186$, see Supplementary Fig. S7), and found similar results. Interestingly, the same analysis on 'target-pre-sac' epoch in visually-guided saccade task showed a significant correlation between hemifield preference in instructed and choice trials ($R = 0.29$, $P = 0.001$, $N=137$), despite the fact that the activity in this epoch represents not only the upcoming saccade preparation but also the visual input that is the same regardless of a choice. These findings suggest that the upcoming spatial decision and movement preparation signals were stronger when the saccade was immediate and to a visual target, whereas the spatially-selective delay period activity can be largely attributed to retrospective memory of visual stimulation or attentional allocation.

Discussion

The goal of this study was to characterize visual-, delay-, and saccade-related properties, as well as choice selectivity of dorsal pulvinar neurons, similar to what has been done extensively for other thalamic nuclei and frontoparietal cortical regions (Funahashi et al. 1991; Barash et al. 1991a, 1991b; Chafee and Goldman-Rakic 1998; Constantinidis et al. 2001; Wyder et al. 2003; Watanabe et al. 2006; Tanaka and Kunimatsu 2011). We utilized a classical memory-guided saccade task to dissociate sensory encoding, intervening delay and motor execution phases, and

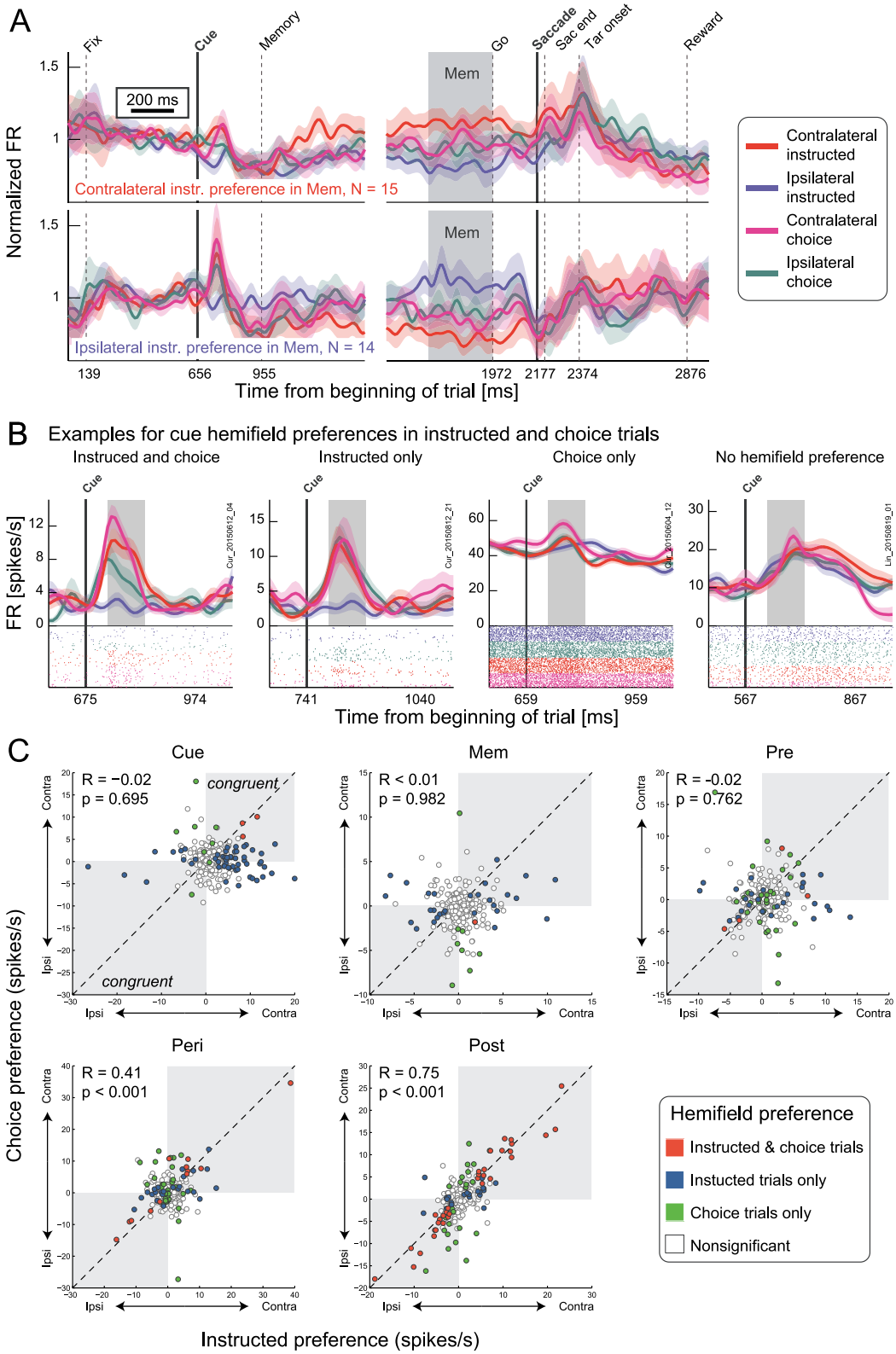

Fig. 9. Spatial choice selectivity. (A) Population averages for 29 units showing either contralateral preference (top) or ipsilateral preference (bottom) in the memory (Mem) epoch, for instructed contralateral (orange) and ipsilateral (blue), choice contralateral (magenta) and ipsilateral (green) trials (compared with Fig. 8I, J, six units were excluded because they were recorded for <24 choice trials to one hemifield). (B) Example units with different types of cue responses, from left to right: contralateral preference in both instructed and choice (CI_{instr} = 0.64, CI_{choice} = 0.329), contralateral preference only in instructed (CI_{instr} = 0.53, CI_{choice} = –0.03), contralateral preference only in choice (CI_{instr} = 0.028, CI_{choice} = 0.075), no hemifield preference (CI_{instr} = –0.03, CI_{choice} = 0.071). (C) Scatter plots comparing firing rate hemifield preference (FR_{contra} – FR_{ipsi}) in instructed and choice trials, for five epochs: cue onset (Cue), memory (Mem), pre-saccadic (Pre), peri-saccadic (Pre), and post-saccadic (Post). *R* and *P*-values are for Pearson's correlations between hemifield preference in instructed and choice trials; congruent tuning quadrants are in gray. Out of 322 units, 36 units were excluded from this analysis because <24 choice trials for one hemifield were recorded (*N*=286).

found a considerable diversity of response patterns. Our results demonstrate that majority of dorsal pulvinar neurons exhibit either enhancement or suppression around or after saccades. Saccade-related responses were mostly post-saccadic, although there were also a number of neurons showing pre- and peri-saccadic modulation. Only a small fraction of neurons responded exclusively to visual stimulation, further supporting the notion that the dorsal pulvinar is involved in oculomotor processing. Delay period activity was mainly characterized by a gradual suppression of firing relative to the initial fixation period, with only a small subset showing classical sustained or ramping up enhancement of activity that is frequently observed in frontoparietal areas such as LIP and FEF. Surprisingly, on the population level no spatial choice selectivity for the upcoming saccade was found, neither in the cue/delay nor in pre-saccadic activity, and individual units rarely showed a consistent spatial tuning across single target instructed and two-target choice trials.

Anatomical considerations

When comparing results presented here with the few previous studies on visual and oculomotor properties of the pulvinar, it is important to note that most studies in the dorsal pulvinar recorded from the dorsomedial division of the *lateral* pulvinar. This division is denoted as PLdm (Kaas and Lyon 2007; Bridge et al. 2016; Kagan et al. 2021), or as Pdm in original electrophysiological studies by Robinson, Petersen and colleagues (e.g. Petersen et al. 1985, 1987; Robinson et al. 1986; Bender and Youakim 2001). The notable exception is a study that covered both lateral and medial parts of the dorsal pulvinar, predominantly at the border between the two (Benevento and Port 1995). Our recording sites were largely within the medial pulvinar (MPul) or around the border between the medial and the lateral pulvinar (see also Dominguez-Vargas et al. 2017; Schneider et al. 2019). We did not observe any clear patterns along the dorsal/lateral-ventral/medial axis in the features we tested, and such patterns have also not been reported in the previous work. However, given rostral-caudal and lateral-medial gradients of dPul anatomical and functional connectivity (Baleydier and Morel 1992; Baizer et al. 1993; Gutierrez et al. 2000; Arcaro et al. 2018; Froesel et al. 2021), more extensive electrophysiological and combined perturbation-imaging mapping (Klink et al. 2021) will be required to further assess the functional differences between subdivisions of the dorsal pulvinar.

Visual and prevalent saccade-related responses

In the memory saccade task, we found diverse patterns of visual and post-saccadic activations along a visual-saccadic continuum, and no clear organization of these patterns within the dorsal pulvinar. Notably, purely visual responses were less frequent than pure post-saccadic responses or combined visual and post-saccadic responses (12% visual compared with 22% visual-saccadic and 30% saccade-related units), supporting an involvement of dorsal pulvinar in distributed neuronal processing related to motor commands and consequences of oculomotor behavior, beyond purely visuospatial functions (Grieve et al. 2000; Guillery and Sherman 2002; Saalmann and Kastner 2015).

Visual responses to a small briefly flashed saccade cue were mainly marked by transient increases of spiking activity, with a clear contralateral preference. This expected presence of cue-related activity contrasts with the previous report in dPul, where responses to visual stimuli were reported only when the stimulus served as a target of an immediate visually-guided saccade but not in memory saccades (Benevento and Port 1995). We indeed found that the combined visual and pre-saccadic activity during visually-guided saccades was stronger than the sum of cue- and pre-saccadic activity during memory saccades—in agreement with the idea that immediate sensorimotor contingency of a stimulus is an important determinant of dPul activity. However, robust cue responses during memory-guided saccades were found in 34% of our sample. The proportion of units, the size of the receptive fields, the range of latencies, and the contralateral tuning of cue responses in dPul are largely consistent with the data from MD, the central thalamus and frontoparietal cortex. This suggests that a pathway via the dorsal pulvinar similar to well-identified cortico–basal ganglia—oculomotor thalamo-cortical loops, an SC—pulvinar, or a direct cortico-pulvinar connectivity, underlie the visual activity in dPul.

The saccade-related responses in dPul show a mix of cortical and other thalamic nuclei properties. In contrast to mainly pre-saccadic activity in MD (Watanabe and Funahashi 2004a; Cavanaugh et al. 2020) and in the central oculomotor thalamus, where saccade-related responses are characterized by equally common space-specific pre-saccadic (47%) and post-saccadic (53%) activity (Wyder et al. 2003), saccade-related responses in dPul are mainly post-saccadic (52% of all units compared with 18% with pre-saccadic activity). But similarly to the central oculomotor thalamus, dPul shows twice as much post-saccadic enhancement as suppression (36 and 16% of all units) relative to the preceding memory delay period. Likewise, a sizable fraction of spatially-tuned post-saccadic enhancement (34%), with only a weak contralateral spatial preference on a population level and extensive RFs that often extend to the ipsilateral side and include the foveal region, resemble the saccadic RFs in the lateral MD and central oculomotor thalamus (Wyder et al. 2003; Cavanaugh et al. 2020). Notably, post-saccadic responses mainly started right after the saccade, before appearance of the confirmation target, and many such responses do not seem to be only a simple consequence of retinal motion-induced visual activation, based on their timing and spatial tuning, as also has been found in the oculomotor thalamus (Wyder et al. 2003).

Both directionally-selective and non-directional (or "omni-directional") post-saccadic enhancement responses are also common in parietal cortex, in LIP and particularly in area 7a (Barash et al. 1991a, 1991b; Genovesio et al. 2007; Zhou et al. 2016b), prefrontal cortex (Funahashi 2014), and the thalamus (Wyder et al. 2003; Tanaka and Kunimatsu 2011). A number of functions related to feedback and internal monitoring have been attributed to these responses. The non-space-specific post-saccadic enhancement could be used for timing, to signal that the saccade has ended and processing of visual inputs can be re-established (Schlag and Schlag-Rey 1984; Tanaka and Kunimatsu 2011; Boi et al. 2017; Kagan and Burr 2017; Zhou et al. 2018). In the context of the memory saccade task, post-saccadic enhancement might also reflect the anticipation of a change in visual input such as the confirmation target onset, since it appears soon after the end of the saccade with a predictable timing. Potentially, deviations of the post-saccadic eye position from the intended target location, i.e. error signals, could also be encoded in post-saccadic responses, as has been found in LIP (Zhou et al. 2016b; Munuera and Duhamel 2020), but the small saccade endpoint dispersion due to fairly stereotypical movements in our experiment did not allow to systematically check for this possibility. Finally, the spatially-tuned post-saccadic responses could also signal the new gaze position, alone or in a combination with previous eye movement vector or pre-saccadic position, and utilized for internal monitoring during

action sequences (Genovesio et al. 2007; Tanaka 2007; Schneider et al. 2019).

The second most frequent saccade-related response in dPul was a transient, typically non-space-specific pre- and peri-saccadic suppression (pre: 9%, peri: 15%,). Some of these neurons also showed a burst after the saccade—similar to so called 'pause-rebound' response found in central thalamus (Tanaka and Kunimatsu 2011). The pre/peri-saccadic suppression could reflect extraretinal signals such as corollary discharge intended to prevent self-induced stimulus motion, e.g. by suppressing visual information transfer to frontoparietal areas during the saccade (Sommer and Wurtz 2004; Bellebaum et al. 2005; Kagan et al. 2008; Ibbotson and Krekelberg 2011; Wurtz et al. 2011a; Wurtz et al. 2011b).

Another subset of units exhibited transient pre-saccadic (9%) and peri-saccadic enhancement (11%), with an overall weak preference for the contralateral hemifield. The activity in these units resembles saccade-related responses in oculomotor thalamus, FEF, and LIP, although such pre/peri-saccadic enhancement is much more prevalent in these regions (Barash et al. 1991a; Wyder et al. 2003; Watanabe et al. 2006). The pre/peri-saccadic response strength in dPul might depend on the behavioral demands and decision urgency, as found in the oculomotor thalamus (Costello et al. 2015). Since we used a fixed memory delay and a relatively generous saccade RT cutoff (500 ms), we surmise that the urgency in our task was low, which might explain a low prevalence of pre/peri-saccadic activity in this dataset.

Delay period activity and choice selectivity

Given the widespread reciprocal connectivity between dorsal pulvinar and the frontoparietal network (Bos and Benevento 1975; Schmahmann and Pandya 1990; Hardy and Lynch 1992), and the fact that dorsal pulvinar perturbation reliably biases saccade target selection during visually-guided and memory-guided saccades (Wilke et al. 2010b, 2013; Dominguez-Vargas et al. 2017), it is important to know if and how dorsal pulvinar activity reflects spatial decisions and movement planning. Memory delay activity modulation was found in 36% of dPul units. Surprisingly, delay period responses were characterized mainly by non-space-specific suppression, rather than the spatially-specific enhancement that is more common in oculomotor thalamus and frontoparietal cortex. In dPul, suppression during the memory period was twice as frequent as enhancement, and in units showing such suppression the activity was often ramping down to a minimum around the go signal, whereas enhancement was typically sustained throughout the memory period.

The gradual decrease in firing rate during the memory period appears to be a complementary pattern to a gradual ramping up/climbing toward the saccade onset often found in frontoparietal cortex (Gnadt and Andersen 1988; Lawrence et al. 2005; Rorie et al. 2010; Premereur et al. 2011; Hwang and Andersen 2012) and in oculomotor thalamus (Watanabe and Funahashi 2004a; Tanaka and Kunimatsu 2011). Of course, the suppression during the memory delay has also been reported in these regions, but it seems to characterize only a minority of neurons (Barash et al. 1991a; Wyder et al. 2003; Watanabe and Funahashi 2004a). Hence, if we assume that the prevalent delay period activity in the frontoparietal cortex is spatially-specific excitation, the suppression in dPul implies inhibitory projections (e.g. directly or via the thalamic reticular nucleus, TRN) from cortex to pulvinar or/and from pulvinar to cortex. It is important to note however that most of the suppression was not spatially-specific, unlike the cortical delay activity; hence, the prevalent patterns in dPul and cortex are not simply an inverse of each other. The non-spatial suppression might be related to a role in general alertness, task attention or non-specific movement preparation rather than specific movement planning. Unlike the "default mode" posterior cingulate neurons where the activity is suppressed starting from the onset of task-related fixation (Hayden et al. 2009), many dPul neurons decrease their firing rate below that in the initial fixation period, following a brief peripheral cue. This is interesting because the visual conditions are the same in the initial fixation and the memory delay epochs (only central fixation point is visible), but the cognitive state is different—expectation of a peripheral visual cue vs. maintenance of spatial information, motor preparation and, at the same time, attention to an upcoming foveal go signal.

Apart from mainly suppressive non-spatial signals, some dPul units (11%) also showed differential memory period responses for upcoming ipsilateral and contralateral instructed saccades, indicating potential involvement in directly linking the visual cue and the upcoming action. There was no contralateral preference of memory activity on a population level, but there was an asymmetry in the two subgroups. The contralaterally-tuned units also showed contralateral cue responses and some ramping enhancement in the end of the delay relative to the fixation baseline. The ipsilaterally-tuned units did not show matching ipsilateral cue responses or ipsilateral ramping, but rather a suppression for contralateral trials. For comparison, 25% of units in central thalamus showed spatially-specific, mainly contralateral delay period activity in a visually-guided delayed saccade task (which is likely to produce stronger delay period activity due to the presence of visual stimulus during the delay), and mostly congruent cue and delay period tuning (Wyder et al. 2003). An even larger fraction of MD units (53%) showed mainly contralateral and cue-congruent excitatory delay period activity (Watanabe and Funahashi 2004a). Less predominant and less contralateral delay period activity sets dPul apart from those oculomotor thalamic nuclei.

Another likely distinction of dPul from the central thalamus and MD is the degree to which these structures show prospective target selection. In rotation or bilateral target color-matching choice memory saccade tasks, many neurons in MD and the central thalamus prospectively encode the direction of the upcoming saccade, rather than visual cues (Wyder et al. 2004; Watanabe and Funahashi 2004b). In contrast, memory period and pre-saccadic activity in spatially selective dPul neurons did not signal the upcoming movement direction during bilateral cue free choice trials. Choice selectivity analysis indicated that target selection was not reflected in the epochs before the saccade onset, because only a very small amount of units significantly preferred the same hemifield in both instructed and choice trials. While it is worth noting that the free choice where both targets are "correct" differs from the above tasks because they unequivocally specify the correct target, it stands to reason that oculomotor thalamus would exhibit a prospective target selection also in the free choice task, as was demonstrated in the frontoparietal cortex (Coe et al. 2002; Watanabe and Funahashi 2007). The lack of congruent (to instructed trials) choice selectivity in dPul suggests that the observed spatial modulation in the instructed trials reflects the retrospective visual processing rather than the spatial decision for the upcoming movement (Lindner et al. 2010; Lundqvist et al. 2018).

The finding that the dPul delay period activity does not encode the upcoming choice might appear to challenge the underlying notion that the pulvinar activity during the memory delay period is directly involved in decision making, derived from the

inactivation studies (Wilke et al. 2010b, 2013). On the other hand, the lack of choice encoding is consistent with our recent findings showing the lack of the choice bias induced by the transient dPul microstimulation during the memory delay, as compared with strong choice effect in the pre-saccadic epoch of the visually-guided task (Dominguez-Vargas et al. 2017). But we emphasize that neither of those findings invalidate the results showing a contralesional choice deficit during memory saccades due to dPul inactivation. Such choice biases are likely caused by disrupting contralesional visual and less prominent pre/peri-saccadic activity, as well as, more hypothetically, the across-trial changes in post-saccadic confidence or feedback evaluation affecting future target selection. Furthermore, since such dPul activity is transmitted to the cortex, the dPul inactivation is expected to strongly affect cortical contralesional spatial representations and ensuing visuomotor decisions (Wilke et al. 2010a; Jaramillo et al. 2019; Klink et al. 2021).

Furthermore, and not mutually exclusive to encoding visuomotor decision and planning, it has been shown that both dorsal and ventral lateral pulvinar causally contribute to orienting spatial attention (Petersen et al. 1987; Desimone et al. 1990; Zhou et al. 2016a). In terms of the underlying neuronal signals, two studies in the ventral lateral pulvinar (Saalmann et al. 2012; Zhou et al. 2016a) and one recent study in the medial dorsal pulvinar (Fiebelkorn et al. 2019) reported slight but significantly enhanced persistent activity during sustained attention to a visible stimulus in the receptive field. It is hence conceivable that the presence of a visual stimulus, which is attended to or is a goal of an upcoming movement, is required for the pulvinar to exhibit the delay period enhancement and spatial selectivity.

Overall, a considerable task-related activity during the delay period notwithstanding, our results strengthen a prior conclusion (Bender and Baizer 1990) that the primary oculomotor role of the pulvinar is not in neural events leading to prospective saccade preparation and generation, at least in the absence of a visible goal (i.e. as in the memory saccade task). Rather, dPul is mainly involved in integrating consequences of saccadic eye movements (saccade direction, amplitude, time of occurrence) with visual processing.

Future directions

The importance of systematic characterization of basic visuomotor properties of a complex and still not well understood structure like the dorsal pulvinar cannot not be overstated. At the same time, the insights gained with simple oculomotor tasks like visually- and memory-guided saccades are inherently limited, given the diversity of pulvinar responses and its proposed involvement in multiple cognitive processes. More elaborate tasks are needed to further evaluate and dissociate involvement of dorsal pulvinar neurons in visual processing, spatial target selection, attentional and motivational factors. One way is to utilize paradigms that dissociate the visual input and the motor output, e.g. anti-saccade or rotated saccade tasks (Munoz and Everling 2004; Watanabe and Funahashi 2004b; Kunimatsu and Tanaka 2010). Second, the tasks that combine immediate stimulus information with a decision urgency, such as the compelled saccade task (Costello et al. 2015) or a difficult perceptual discrimination under a time pressure, might evoke more prospective encoding in the pulvinar neurons. Third, choice tasks with an explicit "correct" response, e.g. color matching target/distractor choice task (Wyder et al. 2004), or with reward modulation where different color targets provide a different amount of reward (Wilke et al. 2013), may inform about the encoding of behavioral salience and selected action.

Beyond the question of target selection in the memory-guided oculomotor task, dPul might be more involved in guiding other movements such as hand actions, as suggested by the effect of pulvinar inactivation or lesions on target selection via reaching and grasping, and hand-specific deficits (Wilke et al. 2010b; Wilke et al. 2018), as well as its strong connectivity to the medial posterior parietal areas (Cappe et al. 2007; Gamberini et al. 2021, 2021). Furthermore, given that many dPul units show gain-field like properties or other types of postural modulations by the position of the eyes in the orbit (Schneider et al. 2019), it remains important to assess if pulvinar is causally involved in spatial reference frame transformations and eye-hand coordination. Rodent studies also suggest that the medial part of the lateral posterior nucleus, the homolog of the primate pulvinar, is connected to amygdala, striatum and frontoparietal cortex and integrates sensorimotor multimodal information, providing an evolutionary perspective on the role of the pulvinar in coordination of perception and body movements (Zhou et al. 2017; Blot et al. 2021; Leow et al. 2022).

A pivotal challenge for ongoing and future research is to link neuronal properties of the pulvinar and other higher-order thalamic nuclei to their circuit-level organization (Sherman 2017). For instance, the memory delay activity in the cortex is in part attributed to local excitatory recurrent connections (Constantinidis et al. 2018; Hart and Huk 2020), whereas the thalamus lacks such connectivity (Halassa and Sherman 2019). This might constrain the expectations about finding persistent working memory/planning activity in the pulvinar, although such activity is abundant in MD, and both pulvinar and MD might help sustain a feature-specific persistent activity in the cortex by regulating the local and inter-areal functional connectivity (Zhou et al. 2016a; Halassa and Kastner 2017). Ultimately, the function of individual pulvinar neurons and microcircuits, and their influence on the cortical processing, is determined by convergent vs. segregated and driving vs. modulatory nature of inputs and outputs (Purushothaman et al. 2012; Bickford 2016; Halassa and Kastner 2017; Sherman 2017; de Souza et al. 2020; Kirchgessner et al. 2021). Therefore, recent advances in neurotransmitter, cell type and pathway-specific dissection of neural circuitry in primates offer great potential for deciphering pulvinar-cortical processing (Kinoshita et al. 2019; Klink et al. 2021; Raper and Galvan 2022; Vanduffel and Isa 2023).

Conclusion

The response timing and tuning suggest that the dorsal pulvinar contributes to spatial actions largely by supporting visuomotor processing around visual cues and saccades. Many neurons show a conjunction of at least two of the three components - visual, delay and/or saccade-related responses. But properties of most individual neurons are inconsistent with prospective transformation of spatial goals into actions during the working memory saccade task. These findings do not rule out more direct involvement of the dorsal pulvinar at the level of single neurons to prospective planning and decision in other contexts. Furthermore, beyond the single neuron perspective, the dorsal pulvinar is well positioned to mediate the visuomotor transformations and spatial decisions at the level of neuronal ensembles comprising groups of neurons encoding different task components, locally and via the connectivity to the cortex.

Acknowledgements

We thank Ira Panolias, Daniela Lazzarini, Sina Plümer, Klaus Heisig, Leonore Burchardt, and Dirk Prüße for technical support.

We thank Stefan Treue, Alexander Gail, Hansjörg Scherberger, members of the Decision and Awareness Group, the Sensorimotor Group, and the Cognitive Neuroscience Laboratory for helpful discussions.

Supplementary material

Supplementary material is available at *Cerebral Cortex* online.

Author contributions

Lukas Schneider (Data curation, Formal analysis, Investigation, Methodology, Software, Visualization, Writing—original draft, Writing—review and editing), Adan-Ulises Dominguez-Vargas (Formal analysis, Investigation, Methodology, Software), Lydia Gibson (Investigation, Methodology), Melanie Wilke (Conceptualization, Funding acquisition, Supervision, Writing—original draft, Writing—review and editing), Igor Kagan (Conceptualization, Data curation, Formal analysis, Funding acquisition, Methodology, Project administration, Software, Supervision, Visualization, Writing—original draft, Writing—review and editing).

Funding

This work was supported by the Hermann and Lilly Schilling Foundation, German Research Foundation (DFG) grants WI 4046/1-1 and Research Unit GA1475-B4, KA 3726/2-1, CNMPB Primate Platform, and core funding from the Cognitive Neuroscience Laboratory, German Primate Center.

Conflict of Interest statement: None declared.

Data availability

The data underlying this article will be shared on reasonable request to the corresponding author.

References

Arcaro MJ, Pinsk MA, Kastner S. The anatomical and functional organization of the human visual pulvinar. *J Neurosci*. 2015:35(27):9848–9871.

Arcaro MJ, Pinsk MA, Chen J, Kastner S. Organizing principles of pulvino-cortical functional coupling in humans. *Nat Commun*. 2018:9(1):5382.

Baizer JS, Desimone R, Ungerleider LG. Comparison of subcortical connections of inferior temporal and posterior parietal cortex in monkeys. *Vis Neurosci*. 1993:10(1):59–72.

Bakker R, Tiesinga P, Kötter R. The Scalable Brain Atlas: instant web-based access to public brain atlases and related content. *Neuroinformatics*. 2015:13(3):353–366.

Baldwin MKL, Balaram P, Kaas JH. The evolution and functions of nuclei of the visual pulvinar in primates. *J Comp Neurol*. 2017:525(15):3207–3226.

Baleydier C, Morel A. Segregated thalamocortical pathways to inferior parietal and inferotemporal cortex in macaque monkey. *Vis Neurosci*. 1992:8(5):391–405.

Barash S, Bracewell RM, Fogassi L, Gnadt JW, Andersen RA. Saccade-related activity in the lateral intraparietal area. I. Temporal properties; comparison with area 7a. *J Neurophysiol*. 1991a:66(3):1095–1108.

Barash S, Bracewell RM, Fogassi L, Gnadt JW, Andersen RA. Saccade-related activity in the lateral intraparietal area. II. Spatial properties. *J Neurophysiol*. 1991b:66(3):1109–1124.

Basso MA, Wurtz RH. Modulation of neuronal activity in superior colliculus by changes in target probability. *J Neurosci*. 1998:18(18):7519–7534.

Bellebaum C, Daum I, Koch B, Schwarz M, Hoffmann KP. The role of the human thalamus in processing corollary discharge. *Brain*. 2005:128(5):1139–1154.

Bender DB, Baizer JS. Saccadic eye movements following kainic acid lesions of the pulvinar in monkeys. *Exp Brain Res*. 1990:79(3):467–478.

Bender DB, Butter CM. Comparison of the effects of superior colliculus and pulvinar lesions on visual search and tachistoscopic pattern discrimination in monkeys. *Exp Brain Res*. 1987:69(1):140–154.

Bender DB, Youakim M. Effect of attentive fixation in macaque thalamus and cortex. *J Neurophysiol*. 2001:85(1):219–234.

Benevento LA, Miller J. Visual responses of single neurons in the caudal lateral pulvinar of the macaque monkey. *J Neurosci*. 1981:1(11):1268–1278.

Benevento LA, Port JD. Single neurons with both form/color differential responses and saccade-related responses in the nonretinotopic pulvinar of the behaving macaque monkey. *Vis Neurosci*. 1995:12(03):523–544.

Benjamini Y, Hochberg Y. Controlling the false discovery rate: a practical and powerful approach to multiple testing. *J R Stat Soc Series B Stat Methodol*. 1995:57(1):289–300.

Berger M, Calapai A, Stephan V, Niessing M, Burchardt L, Gail A, Treue S. Standardized automated training of rhesus monkeys for neuroscience research in their housing environment. *J Neurophysiol*. 2018:119(3):796–807.

Berman RA, Wurtz RH. Signals conveyed in the pulvinar pathway from superior colliculus to cortical area MT. *J Neurosci*. 2011:31(2):373–384.

Bickford ME. Thalamic circuit diversity: modulation of the driver/-modulator framework. *Front Neural Circuits*. 2016:9.

Bisley JW, Goldberg ME. Attention, intention, and priority in the parietal lobe. *Annu Rev Neurosci*. 2010:33:1–21.

Blot A, Roth MM, Gasler I, Javadzadeh M, Imhof F, Hofer SB. Visual intracortical and transthalamic pathways carry distinct information to cortical areas. *Neuron*. 2021:109(12):1996–2008.

Boi M, Poletti M, Victor JD, Rucci M. Consequences of the oculomotor cycle for the dynamics of perception. *Curr Biol*. 2017:27(9):1268–1277.

Bos J, Benevento LA. Projections of the medial pulvinar to orbital cortex and frontal eye fields in the rhesus monkey (Macaca mulatta). *Exp Neurol*. 1975:49(2):487–496.

Bourgeois A, Guedj C, Carrera E, Vuilleumier P. Pulvino-cortical interaction: an integrative role in the control of attention. *Neurosci Biobehav Rev*. 2020:111:104–113.

Brainard DH. The Psychophysics Toolbox. *Spat Vis*. 1997:10:433–436.

Bridge H, Leopold DA, Bourne JA. Adaptive pulvinar circuitry supports visual cognition. *Trends Cogn Sci*. 2016:20(2):146–157.

Bruce CJ, Goldberg ME. Primate frontal eye fields. I. Single neurons discharging before saccades. *J Neurophysiol*. 1985:53(3):603–635.

Calapai A, Berger M, Niessing M, Heisig K, Brockhausen R, Treue S, Gail A. A cage-based training, cognitive testing and enrichment system optimized for rhesus macaques in neuroscience research. *Behav Res Methods*. 2017:49(1):35–45.

Cappe C, Morel A, Rouiller EM. Thalamocortical and the dual pattern of corticothalamic projections of the posterior parietal cortex in macaque monkeys. *Neuroscience*. 2007:146(3):1371–1387.

Cavanaugh J, McAlonan K, Wurtz RH. Organization of corollary discharge neurons in monkey medial dorsal thalamus. *J Neurosci*. 2020:40(33):6367–6378.

Chafee MV, Goldman-Rakic PS. Matching patterns of activity in primate prefrontal area 8a and parietal area 7ip neurons during a spatial working memory task. *J Neurophysiol*. 1998:79(6): 2919–2940.

Chen M, Li B, Guang J, Wei L, Wu S, Liu Y, Zhang M. Two subdivisions of macaque LIP process visual-oculomotor information differently. *Proc Natl Acad Sci*. 2016:113(41):E6263–E6270.

Coe B, Tomihara K, Matsuzawa M, Hikosaka O. Visual and anticipatory bias in three cortical eye fields of the monkey during an adaptive decision-making task. *J Neurosci*. 2002:22(12): 5081–5090.

Colby CL, Duhamel JR, Goldberg ME. Visual, presaccadic, and cognitive activation of single neurons in monkey lateral intraparietal area. *J Neurophysiol*. 1996:76(5):2841–2852.

Constantinidis C, Franowicz MN, Goldman-Rakic PS. The sensory nature of mnemonic representation in the primate prefrontal cortex. *Nat Neurosci*. 2001:4(3):311–316.

Constantinidis C, Funahashi S, Lee D, Murray JD, Qi XL, Wang M, Arnsten AFT. Persistent spiking activity underlies working memory. *J Neurosci*. 2018:38(32):7020–7028.

Costello MG, Zhu D, May PJ, Salinas E, Stanford TR. Task dependence of decision- and choice-related activity in monkey oculomotor thalamus. *J Neurophysiol*. 2015:115(1):581–601.

Dean HL, Crowley JC, Platt ML. Visual and saccade-related activity in macaque posterior cingulate cortex. *J Neurophysiol*. 2004:92(5): 3056–3068.

Desimone R, Wessinger M, Thomas L, Schneider W. Attentional control of visual perception: cortical and subcortical mechanisms. *Cold Spring Harb Symp Quant Biol*. 1990:55:963–971.

Dominguez-Vargas AU, Schneider L, Wilke M, Kagan I. Electrical microstimulation of the pulvinar biases saccade choices and reaction times in a time-dependent manner. *J Neurosci*. 2017:37(8): 2234–2257.

Fiebelkorn IC, Pinsk MA, Kastner S. The mediodorsal pulvinar coordinates the macaque fronto-parietal network during rhythmic spatial attention. *Nat Commun*. 2019:10(1):215.

Froesel M, Cappe C, Ben HS. A multisensory perspective onto primate pulvinar functions. *Neurosci Biobehav Rev*. 2021:125:231–243.

Funahashi S. Saccade-related activity in the prefrontal cortex: its role in eye movement control and cognitive functions. *Front Integr Neurosci*. 2014:8.

Funahashi S, Bruce CJ, Goldman-Rakic PS. Neuronal activity related to saccadic eye movements in the monkey's dorsolateral prefrontal cortex. *J Neurophysiol*. 1991:65(6):1464–1483.

Gamberini M, Passarelli L, Filippini M, Fattori P, Galletti C. Vision for action: thalamic and cortical inputs to the macaque superior parietal lobule. *Brain Struct Funct*. 2021:226(9):2951–2966.

Genovesio A, Brunamonti E, Giusti MA, Ferraina S. Postsaccadic activities in the posterior parietal cortex of primates are influenced by both eye movement vectors and eye position. *J Neurosci*. 2007:27(12):3268–3273.

Gnadt JW, Andersen RA. Memory related motor planning activity in posterior parietal cortex of macaque. *Exp Brain Res*. 1988:70: 216–220.

Grieve KL, Acuña C, Cudeiro J. The primate pulvinar nuclei: vision and action. *Trends Neurosci*. 2000:23(1):35–39.

Guillery RW, Sherman SM. The thalamus as a monitor of motor outputs. *Philos Trans R Soc Lond B Biol Sci*. 2002:357(1428):1809–1821.

Gutierrez C, Cola MG, Seltzer B, Cusick C. Neurochemical and connectional organization of the dorsal pulvinar complex in monkeys. *J Comp Neurol*. 2000:419(1):61–86.

Halassa MM, Kastner S. Thalamic functions in distributed cognitive control. *Nat Neurosci*. 2017:20(12):1669–1679.

Halassa MM, Sherman SM. Thalamocortical circuit motifs: a general framework. *Neuron*. 2019:103(5):762–770.

Hardy SGP, Lynch JC. The spatial distribution of pulvinar neurons that project to two subregions of the inferior parietal lobule in the macaque. *Cereb Cortex*. 1992:2(3):217–230.

Hart E, Huk AC. Recurrent circuit dynamics underlie persistent activity in the macaque frontoparietal network. *eLife*. 2020:9:e52460.

Hayden BY, Smith DV, Platt ML. Electrophysiological correlates of default-mode processing in macaque posterior cingulate cortex. *Proc Natl Acad Sci*. 2009:106(14):5948–5953.

Hikosaka O, Wurtz RH. Visual and oculomotor functions of monkey substantia nigra pars reticulata. III. Memory-contingent visual and saccade responses. *J Neurophysiol*. 1983:49(5):1268–1284.

Homman-Ludiye J, Mundinano IC, Kwan WC, Bourne JA. Extensive connectivity between the medial pulvinar and the cortex revealed in the marmoset monkey. *Cereb Cortex*. 2020:30(3): 1797–1812.

Hwang EJ, Andersen RA. Spiking and LFP activity in PRR during symbolically instructed reaches. *J Neurophysiol*. 2012:107(3):836–849.

Ibbotson M, Krekelberg B. Visual perception and saccadic eye movements. *Curr Opin Neurobiol*. 2011:21(4):553–558.

Ipata AE, Gee AL, Goldberg ME, Bisley JW. Activity in the lateral intraparietal area predicts the goal and latency of saccades in a free-viewing visual search task. *J Neurosci*. 2006:26(14):3656–3661.

Jaramillo J, Mejias JF, Wang XJ. Engagement of pulvino-cortical feedforward and feedback pathways in cognitive computations. *Neuron*. 2019:101(2):321–336.e9.

Kaas JH, Baldwin MKL. The evolution of the pulvinar complex in primates and its role in the dorsal and ventral streams of cortical processing. *Vision*. 2020:4(1):3.

Kaas JH, Lyon DC. Pulvinar contributions to the dorsal and ventral streams of visual processing in primates. *Brain Res Rev*. 2007:55(2): 285–296.

Kagan I, Burr DC. Active vision: dynamic reformatting of visual information by the saccade-drift cycle. *Curr Biol*. 2017:27(9):R341–R344.

Kagan I, Gur M, Snodderly DM. Saccades and drifts differentially modulate neuronal activity in V1: effects of retinal image motion, position, and extraretinal influences. *J Vis*. 2008:8(14):19–19.

Kagan I, Iyer A, Lindner A, Andersen RA. Space representation for eye movements is more contralateral in monkeys than in humans. *Proc Natl Acad Sci*. 2010:107(17):7933–7938.

Kagan I, Gibson L, Spanou E, Wilke M. Effective connectivity and spatial selectivity-dependent fMRI changes elicited by microstimulation of pulvinar and LIP. *NeuroImage*. 2021:240:118283.

Kinoshita M, Kato R, Isa K, Kobayashi K, Kobayashi K, Onoe H, Isa T. Dissecting the circuit for blindsight to reveal the critical role of pulvinar and superior colliculus. *Nat Commun*. 2019:10(135): 1–10.

Kirchgessner MA, Franklin AD, Callaway EM. Distinct "driving" versus "modulatory" influences of different visual corticothalamic pathways. *Curr Biol*. 2021:31(23):5121–5137.e7.

Klaes C, Westendorff S, Chakrabarti S, Gail A. Choosing goals, not rules: deciding among rule-based action plans. *Neuron*. 2011:70(3):536–548.

Klink PC, Aubry JF, Ferrera VP, Fox AS, Froudist-Walsh S, Jarraya B, Konofagou EE, Krauzlis RJ, Messinger A, Mitchell AS, et al. Combining brain perturbation and neuroimaging in non-human primates. *NeuroImage*. 2021:235:118017.

Komura Y, Nikkuni A, Hirashima N, Uetake T, Miyamoto A. Responses of pulvinar neurons reflect a subject's confidence in visual categorization. *Nat Neurosci*. 2013:16(6):749–755.

Kunimatsu J, Tanaka M. Roles of the primate motor thalamus in the generation of antisaccades. *J Neurosci*. 2010:30(14):5108–5117.

Lawrence BM, White RL, Snyder LH. Delay-period activity in visual, visuomovement, and movement neurons in the frontal eye field. *J Neurophysiol*. 2005:94(2):1498–1508.

Leow YN, Zhou B, Sullivan HA, Barlowe AR, Wickersham IR, Sur M. Brain-wide mapping of inputs to the mouse lateral posterior (LP/pulvinar) thalamus–anterior cingulate cortex network. *J Comp Neurol*. 2022:530(11):1992–2013.

Lindner A, Iyer A, Kagan I, Andersen RA. Human posterior parietal cortex plans where to reach and what to avoid. *J Neurosci*. 2010:30(35):11715–11725.

Lundqvist M, Herman P, Miller EK. Working memory: delay activity, yes! Persistent activity? Maybe Not. *J Neurosci*. 2018:38(32):7013–7019.

Maris E, Oostenveld R. Nonparametric statistical testing of EEG- and MEG-data. *J Neurosci Methods*. 2007:164(1):177–190.

Mirpour K, Bisley JW. Remapping, spatial stability, and temporal continuity: from the pre-saccadic to postsaccadic representation of visual space in LIP. *Cereb Cortex*. 2016:26(7):3183–3195.

Munoz DP, Everling S. Look away: the anti-saccade task and the voluntary control of eye movement. *Nat Rev Neurosci*. 2004:5(3):218–228.

Munuera J, Duhamel JR. The role of the posterior parietal cortex in saccadic error processing. *Brain Struct Funct*. 2020:225(2):763–784.

Ohayon S, Tsao DY. MR-guided stereotactic navigation. *J Neurosci Methods*. 2012:204(2):389–397.

Pastor-Bernier A, Cisek P. Neural correlates of biased competition in premotor cortex. *J Neurosci*. 2011:31(19):7083–7088.

Petersen SE, Robinson DL, Keys W. Pulvinar nuclei of the behaving rhesus monkey: visual responses and their modulation. *J Neurophysiol*. 1985:54(4):867–886.

Petersen SE, Robinson DL, Morris JD. Contributions of the pulvinar to visual spatial attention. *Neuropsychologia*. 1987:25(1):97–105.

Premereur E, Vanduffel W, Janssen P. Functional heterogeneity of macaque lateral intraparietal neurons. *J Neurosci*. 2011:31(34):12307–12317.

Purushothaman G, Marion R, Li K, Casagrande VA. Gating and control of primary visual cortex by pulvinar. *Nat Neurosci*. 2012:15(6):905–912.

Raper J, Galvan A. Applications of chemogenetics in non-human primates. *Curr Opin Pharmacol*. 2022:64:102204.

Robinson DL, Petersen SE, Keys W. Saccade-related and visual activities in the pulvinar nuclei of the behaving rhesus monkey. *Exp Brain Res*. 1986:62(3): 625–634.

Rohlfing T, Kroenke CD, Sullivan EV, Dubach MF, Bowden DM, Grant K, Pfefferbaum A. The INIA19 template and NeuroMaps atlas for primate brain image parcellation and spatial normalization. *Front Neuroinform*. 2012:6:27.

Rorie AE, Gao J, McClelland JL, Newsome WT. Integration of sensory and reward information during perceptual decision-making in lateral intraparietal cortex (LIP) of the macaque monkey. *PLoS One*. 2010:5(2):e9308.

Saalmann YB, Kastner S. Cognitive and perceptual functions of the visual thalamus. *Neuron*. 2011:71(2):209–223.

Saalmann YB, Kastner S. The cognitive thalamus. *Front Syst Neurosci*. 2015:9:39.

Saalmann YB, Pinsk MA, Wang L, Li X, Kastner S. The pulvinar regulates information transmission between cortical areas based on attention demands. *Science*. 2012:337(6095):753–756.

Schlag J, Schlag-Rey M. Visuomotor functions of central thalamus in monkey. II. Unit activity related to visual events, targeting, and fixation. *J Neurophysiol*. 1984:51(6):1175–1195.

Schmahmann JD, Pandya DN. Anatomical investigation of projections from thalamus to posterior parietal cortex in the rhesus monkey: a WGA-HRP and fluorescent tracer study. *J Comp Neurol*. 1990:295(2):299–326.

Schneider L, Dominguez-Vargas AU, Gibson L, Kagan I, Wilke M. Eye position signals in the dorsal pulvinar during fixation and goal-directed saccades. *J Neurophysiol*. 2019:123(1):367–391.

Sherman SM. Functioning of circuits connecting thalamus and cortex. In: Terjung R, editors. *Comprehensive Physiology*. 1st ed. Wiley; 2017. pp. 713–739. https://onlinelibrary.wiley.com/action/showCitFormats?doi=10.1002/cphy.c160032.

Sommer MA, Wurtz RH. What the brain stem tells the frontal cortex. I. Oculomotor signals sent from superior colliculus to frontal eye field via mediodorsal thalamus. *J Neurophysiol*. 2004:91(3):1381–1402.

de Souza BOF, Cortes N, Casanova C. Pulvinar modulates contrast responses in the visual cortex as a function of cortical hierarchy. *Cereb Cortex*. 2020:30(3):1068–1086.

Stepniewska I, Preuss TM, Kaas JH. Thalamic connections of the primary motor cortex (M1) of owl monkeys. *J Comp Neurol*. 1994:349(4):558–582.

Suriya-Arunroj L, Gail A. Complementary encoding of priors in monkey frontoparietal network supports a dual process of decision-making. *eLife*. 2019:8:e47581.

Tanaka M. Spatiotemporal properties of eye position signals in the primate central thalamus. *Cereb Cortex*. 2007:17(7):1504–1515.

Tanaka M, Kunimatsu J. *Thalamic Roles in Eye Movements*. In: Liversedge SP, Gilchrist I, and Everling S. (eds), The Oxford Handbook of Eye Movements, Oxford Library of Psychology, Oxford University Press; 2011. https://doi.org/10.1093/oxfordhb/9780199539789.001.0001.

Trojanowski JQ, Jacobson S. Areal and laminar distribution of some pulvinar cortical efferents in rhesus monkey. *J Comp Neurol*. 1976:169(3):371–391.

Ungerleider LG, Christensen CA. Pulvinar lesions in monkeys produce abnormal eye movements during visual discrimination training. *Brain Res*. 1977:136(1):189–196.

Vanduffel W, Isa T. Pathway-selective reversible perturbations using a double-infection technique in the macaque brain. In: Eldridge MAG, Galvan A, (eds). *Vectorology for Optogenetics and Chemogenetics*. Springer US: Neuromethods; 2023. pp. 185–205. https://link.springer.com/book/10.1007/978-1-0716-2918-5.

Watanabe Y, Funahashi S. Neuronal activity throughout the primate mediodorsal nucleus of the thalamus during oculomotor delayed-responses. I. Cue-, delay-, and response-period activity. *J Neurophysiol*. 2004a:92(3):1738–1755.

Watanabe Y, Funahashi S. Neuronal activity throughout the primate mediodorsal nucleus of the thalamus during oculomotor delayed-responses. II. Activity encoding visual versus motor signal. *J Neurophysiol*. 2004b:92(3):1756–1769.

Watanabe K, Funahashi S. Prefrontal delay-period activity reflects the decision process of a saccade direction during a free-choice ODR task. *Cereb Cortex*. 2007:17(Suppl 1):i88–i100.

Watanabe K, Igaki S, Funahashi S. Contributions of prefrontal cue-, delay-, and response-period activity to the decision process of saccade direction in a free-choice ODR task. *Neural Netw*. 2006:19(8):1203–1222.

Wilke M, Kagan I, Andersen RA. Pulvinar inactivation alters cortical responses during spatial decision making. In: *280.11/SS19 Neuroscience Meeting Planner*; Society for Neuroscience Annual Meeting 2010a

Wilke M, Turchi J, Smith K, Mishkin M, Leopold DA. Pulvinar inactivation disrupts selection of movement plans. *J Neurosci*. 2010b:30(25):8650–8659.

Wilke M, Kagan I, Andersen RA. Effects of pulvinar inactivation on spatial decision-making between equal and asymmetric reward options. *J Cogn Neurosci*. 2013:25(8):1270–1283.

Wilke M, Schneider L, Dominguez-Vargas AU, Schmidt-Samoa C, Miloserdov K, Nazzal A, Dechent P, Cabral-Calderin Y, Scherberger H, Kagan I, et al. Reach and grasp deficits following damage to the dorsal pulvinar. *Cortex*. 2018:99:135–149.

Wurtz RH, Joiner WM, Berman RA. Neuronal mechanisms for visual stability: progress and problems. *Philos Trans R Soc Lond B Biol Sci*. 2011a:366(1564):492–503.

Wurtz RH, McAlonan K, Cavanaugh J, Berman RA. Thalamic pathways for active vision. *Trends Cogn Sci*. 2011b:15(4):177–184.

Wyder MT, Massoglia DP, Stanford TR. Quantitative assessment of the timing and tuning of visual-related, saccade-related, and delay period activity in primate central thalamus. *J Neurophysiol*. 2003:90(3):2029–2052.

Wyder MT, Massoglia DP, Stanford TR. Contextual modulation of central thalamic delay-period activity: representation of visual and saccadic goals. *J Neurophysiol*. 2004:91(6):2628–2648.

Zhou H, Schafer RJ, Desimone R. Pulvinar-cortex interactions in vision and attention. *Neuron*. 2016a:89(1):209–220.

Zhou Y, Liu Y, Lu H, Wu S, Zhang M. Neuronal representation of saccadic error in macaque posterior parietal cortex. *eLife*. 2016b:5:e10912.

Zhou N, Maire PS, Masterson SP, Bickford ME. The mouse pulvinar nucleus: organization of the tectorecipient zones. *Vis Neurosci*. 2017:34:E11. https://doi.org/10.1017/S0952523817000050.

Zhou Y, Liu Y, Wu S, Zhang M. Neuronal representation of the saccadic timing signals in macaque lateral intraparietal area. *Cereb Cortex*. 2018:28(8):2887–2900.